Cyclin E overexpression impairs progression through mitosis by inhibiting APC^{Cdh1}

Jamie M. Keck,[1] Matthew K. Summers,[2] Donato Tedesco,[1] Susanna Ekholm-Reed,[1] Li-Chiou Chuang,[1] Peter K. Jackson,[2] and Steven I. Reed[1]

[1]Department of Molecular Biology, The Scripps Research Institute, La Jolla, CA 92037
[2]Department of Pathology, Stanford University School of Medicine, Stanford, CA 94305

Overexpression of cyclin E, an activator of cyclin-dependent kinase 2, has been linked to human cancer. In cell culture models, the forced expression of cyclin E leads to aneuploidy and polyploidy, which is consistent with a direct role of cyclin E overexpression in tumorigenesis. In this study, we show that the overexpression of cyclin E has a direct effect on progression through the latter stages of mitotic prometaphase before the complete alignment of chromosomes at the metaphase plate. In some cases, such cells fail to divide chromosomes, resulting in polyploidy. In others, cells proceed to anaphase without the complete alignment of chromosomes. These phenotypes can be explained by an ability of overexpressed cyclin E to inhibit residual anaphase-promoting complex (APC^{Cdh1}) activity that persists as cells progress up to and through the early stages of mitosis, resulting in the abnormal accumulation of APC^{Cdh1} substrates as cells enter mitosis. We further show that the accumulation of securin and cyclin B1 can account for the cyclin E–mediated mitotic phenotype.

Introduction

Cyclin E, an activator of cyclin-dependent kinase (Cdk) 2, accumulates at the G1/S boundary of the cell cycle, where it stimulates functions associated with entry into and progression through S phase (Resnitzky et al., 1994; Ohtsubo et al., 1995; Sauer and Lehner, 1995; Ekholm and Reed, 2000). Normally, cyclin E levels are tightly regulated so that peak cyclin E–Cdk2 kinase activity occurs only for a short interval near the G1/S boundary (Ekholm and Reed, 2000). This is accomplished primarily by the periodic E2F-dependent transcription of cyclin E during late G1 phase (Koff et al., 1991; Dulic et al., 1992) and its subsequent phosphorylation-dependent ubiquitin-mediated proteolysis in S phase when cyclin E–Cdk2 complexes become active (Strohmaier et al., 2001). Cyclin E expression and activation of Cdk2 at the G1/S boundary are compatible with the known roles of cyclin E in the promotion of replication-associated functions (Arata et al., 2000; Geng et al., 2003; Ekholm-Reed et al., 2004a; Mailand and Diffley, 2005).

Correspondence to Steven I. Reed: sreed@scripps.edu

M.K. Summers' and P.K. Jackson's present address is Genentech, Inc., South San Francisco, CA 94080.

D. Tedesco's present address is Berlex, Inc., Richmond, CA 94806.

Abbreviations used in this paper: APC, anaphase-promoting complex; Cdk, cyclin-dependent kinase; EV, empty vector; IME, immortalized mammary epithelial; WT, wild type.

The online version of this article contains supplemental material.

The overexpression of cyclin E has been observed in a broad spectrum of human malignancies, suggesting that proper regulation of cyclin E is important for the preservation of normal cellular functions (Keyomarsi et al., 1995; Sandhu and Slingerland, 2000; Spruck et al., 2002; Erlandsson et al., 2003; Ekholm-Reed et al., 2004b). Under such circumstances, cyclin E is often expressed at levels higher than those observed in normal tissues, but also the periodic expression at the G1/S boundary is frequently lost, with cyclin E levels maintained throughout the cell cycle. This can occur through a single mutation in Cdc4 (also known as Fbw7), the F-box component of an SCF (Skp1-Cul1–F-box protein) ubiquitin ligase that targets cyclin E for ubiquitin-mediated degradation (Strohmaier et al., 2001; Spruck et al., 2002; Rajagopalan et al., 2004). Furthermore, the overexpression of cyclin E in some cancers has been associated with aggressive disease and poor outcome (Dutta et al., 1995; Porter et al., 1997; Nielsen et al., 1998; Erlanson and Landberg, 2001; Keyomarsi et al., 2002). A direct causal link between cyclin E overexpression and tumorigenesis is supported by a transgenic mouse model in which the ectopic expression of cyclin E in the mammary epithelium induces mammary carcinogenesis (Bortner and Rosenberg, 1997; Smith et al., 2006).

The basis for cyclin E–induced tumorigenesis remains controversial. Because cyclin E, by virtue of its ability to activate Cdk2, is a positive regulator of the cell cycle, it has been

© The Rockefeller University Press $15.00
The Journal of Cell Biology, Vol. 178, No. 3, July 30, 2007 371–385
http://www.jcb.org/cgi/doi/10.1083/jcb.200703202

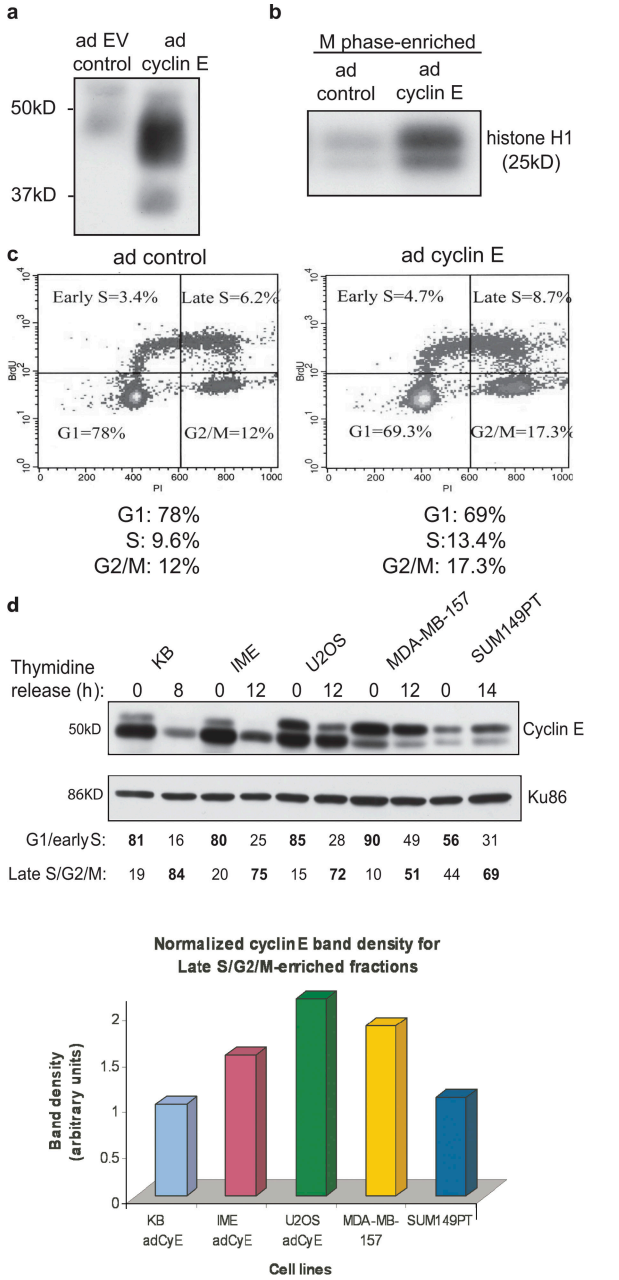

Figure 1. **Cyclin E overexpression and elevated kinase activity leads to an accumulation of S and G2/M populations.** (a) Western blot comparing the expression of cyclin E in KB cells 24 h after transduction with an adenovirus expressing WT cyclin E (ad cyclin E) or with empty vector (EV control). (b) Histone H1 kinase assay of cyclin E–Cdk2 from M-phase enriched cells. KB cells were transduced with cyclin E or EV control adenovirus and weren enriched for mitotic cells using a single thymidine block followed by an 8-h release in the presence of nocodazole. Cell lysates were immunoprecipitated with anti-Cdk2, and the immune complexes were subjected to an in vitro kinase assay using purified histone H1 as a substrate. (c) Cell cycle analysis of adenovirus-transduced KB cells by 2D flow cytometry. Asynchronous KB cells were transduced with cyclin E or EV control adenovirus for 24 h followed by a 20-min incubation with BrdU and were stained with propidium iodide to determine the DNA content and with anti-BrdU antibody to resolve the S-phase population. (d) Comparison of cyclin E levels during the cell cycle between adenovirally transduced cell lines used in this study (KB, IME, and U2OS) and breast cancer–derived cell lines expressing high levels of cyclin E (MDA-MB-157 and SUM149-PT). All adenoviral transductions were performed as described in Materials and methods. Transduced and untransduced cells were subjected to a single thymidine block and release as described in Materials and methods. Cells were collected at the thymidine block and then at 8, 12, and 14 h to find the point with the maximum percentage of cells in late S/G2/M phase (in which cyclin E exerts effects on mitosis). The thymidine-arrested and peak S/G2/M samples were then compared on the same blot for cyclin E levels for all transduced and untransduced cell lines. Cyclin E levels for late S/G2/M-phase enriched fractions or normalized to levels of the invariant nuclear protein Ku86 are plotted below. Cyclin E in cyclin E–transduced KB cells is arbitrarily set to 1.0.

proposed that the role of cyclin E in tumorigenesis is to stimulate cellular proliferation (Geng et al., 2003). This is consistent with the role of cyclin E–Cdk2 in phosphorylating and inactivating the retinoblastoma protein Rb, a negative regulator of proliferation (Lukas et al., 1997; Harbour et al., 1999; Zhang et al., 1999). Furthermore, the ectopic expression of cyclin E was shown to drive cultured cells from G1 into S phase with accelerated kinetics (Ohtsubo and Roberts, 1993; Resnitzky et al., 1994). However, in these studies, the overall rate of proliferation was not altered, arguing against a direct link between cyclin E overexpression and increased proliferation in the context of tumorigenesis. On the other hand, cyclin E–mediated mammary hyperplasia was observed in mice carrying a mammary epithelium–specific cyclin E transgene, which is consistent with a link between cyclin E overexpression and cellular proliferation in vivo (Bortner and Rosenberg, 1997).

An alternative view of the role of cyclin E overexpression in tumorigenesis comes from a study of genomic instability (Spruck et al., 1999). In cultured nontransformed cells, the overexpression of cyclin E led to both chromosome instability and polyploidy (Spruck et al., 1999). Chromosome instability was a relatively infrequent event under moderate levels of cyclin E overexpression but was manifest reproducibly as both chromosome losses and gains, suggesting nondisjunction or other mitotic aberrations as possible mechanisms. Polyploidy was a more frequent event that was easily scorable under the experimental conditions. Polyploid cells, which are themselves unstable, can readily give rise to aneuploidy (Thiagalingam et al., 2000). Cyclin E overexpression in a tissue culture model has also been associated with the formation of micronuclei, which is suggestive of the generation of aneuploid cells (Rajagopalan et al., 2004). Genomic instability in the forms of both chromosome instability and polyploidy, leading to aneuploidy, could easily explain the link between cyclin E overexpression and tumorigenesis.

Genomic instability has been shown to promote tumorigenesis on several levels, most notably by facilitating the loss of heterozygosity at tumor suppressor loci and amplification of oncogenes (Thiagalingam et al., 2000). Consistent with this interpretation, early loss of the heterozygosity of the tumor suppressor gene encoding p53 was observed in the mouse mammary cyclin E transgenic model (Smith et al., 2006). Importantly, both aneuploidy and polyploidy have been observed in human tumors in which cyclin E is overexpressed (Hubalek et al., 2004).

In terms of the mechanism whereby cyclin E overexpression promotes genomic instability, cell cycle analysis has provided several clues. Early studies indicated that the ectopic expression of cyclin E, although accelerating entry into S phase, caused a substantial prolongation of S phase (Ohtsubo and

Roberts, 1993; Resnitzky et al., 1994). A more recent analysis revealed that the overexpression of cyclin E specifically impairs the assembly of prereplication complexes upon mitotic exit, leading to slow and inefficient DNA replication and most likely replicative stress (Ekholm-Reed et al., 2004a). It is easy to envisage how replication defects can lead to genomic instability. In another study in which the cyclin E–targeting F-box protein Cdc4 was mutated in cultured cells, impairing cyclin E turnover, mitotic aberrations in some cells were observed by time-lapse videomicroscopy (Rajagopalan et al., 2004). However, this study could not distinguish between direct effects on mitosis and indirect effects accruing as a result of replicative stress, and because SCF^{Cdc4} also targets other cellular regulatory proteins, the effects could not be definitively attributed to cyclin E overexpression.

In this study, we investigate whether cyclin E overexpression can have a direct impact on the progression through and the quality of mitosis. By expressing cyclin E in a manner that precludes effects on prereplication complex assembly, we demonstrate that the overexpression of cyclin E expression both delays progression through early phases of mitosis and causes mitosis to be executed aberrantly in many cells. Furthermore, we demonstrate that these effects are mediated by the direct action of cyclin E–Cdk2 on protein complexes that regulate mitotic progression.

Results

Deregulating cyclin E expression in cultured cells

To study the acute effects of cyclin E overexpression, a recombinant adenovirus expressing wild-type (WT) cyclin E from the constitutive cytomegalovirus promoter was constructed (Ekholm-Reed et al., 2004a). As shown by Western blotting (Fig. 1 a), KB cells 24 h after transduction with cyclin E adenovirus (Fig. 1 a, ad cyclin E) have increased cyclin E expression compared with cells transduced with an empty vector control adenovirus (Fig. 1 a, ad empty vector [EV] control). Although this ectopically expressed cyclin E exhibits some cell cycle–dependent regulation, levels are substantially higher than WT at all cell cycle phases (Fig. S1, available at http://www.jcb.org/cgi/content/full/jcb.200703202/DC1). To confirm that the adenoviral expression of cyclin E resulted in the elevation of cyclin E–Cdk2 kinase activity with respect to the cell cycle, kinase assays were performed on extracts from mitotic cells, where cyclin E is not normally expressed. KB cells were synchronized using a single thymidine block at the G1/S boundary and were released for 8 h into nocodazole (see Fig. 5 a). Cyclin E–Cdk2 kinase activity in immunoprecipitates was detectable well above background in mitotically enriched extracts after transduction with the cyclin E–expressing adenovirus (Fig. 1 b). The level of cyclin E expression throughout the cell cycle in the adenovirally transduced cell lines used in the current study is equivalent to that characteristic of a subpopulation of breast cancer–derived cell lines that were shown previously to express high levels of cyclin E (Fig. 1 d; Ekholm-Reed et al., 2004a).

Cyclin E overexpression leads to an early mitotic delay

Flow cytometry was used to screen for cell cycle abnormalities resulting from cyclin E overexpression. Previous studies have shown that cells overexpressing cyclin E accumulate in S phase (Ohtsubo and Roberts, 1993; Resnitzky et al., 1994; Ekholm-Reed et al., 2004a). FACS profiles of asynchronous cyclin E and control adenovirus-transduced cells confirmed this observation but also revealed an increase in G2/M cells (Fig. 1 c; ad cyclin E = 17.3% and ad control = 12%).

The aforementioned flow cytometry experiments revealed an accumulation of cells with 4C DNA content. However, these experiments were unable to distinguish G2 from mitotic populations. Immunostaining cells with an antibody reactive with phosphorylated histone H3 (H3-P) produces a distinct punctate pattern beginning at centromeres in G2 cells and brightly covering entire chromosomes in mitotic cells (Hendzel et al., 1997). Fig. 2 a demonstrates the nuclear pattern associated with G2 cells. The onset of histone H3 phosphorylation in U2OS cells was confirmed to begin in late S phase to early G2 by labeling cells with both anti–H3-P and anti-BrdU antibodies after a short BrdU pulse (unpublished data). Scoring interphase U2OS cells for positive H3-P staining demonstrated a decreased G2 population in cyclin E adenovirus-transduced cells (Fig. 2 a; ad control = 12% and ad cyclin E = 6%). This decrease in the fraction of G2 cells indicates that the 4C (G2 + M) accumulation, which was previously shown by FACS analysis in cells overexpressing cyclin E, must be the result of an accumulation of cells in mitosis rather than in G2.

To determine whether cyclin E overexpression leads to the accumulation of cells at a particular stage of mitosis, the distribution of mitotic phases was scored in asynchronous populations using immunofluorescence microscopy. KB cells were transduced with cyclin E or control adenovirus for 24 h, fixed, and immunostained with anti–H3-P to highlight mitotic cells and anti–α-tubulin to label mitotic spindles. Mitotic phases were then scored based on the positions of chromosomes and the orientation of the mitotic spindle. Six mitotic phases were classified and scored in the analysis: prophase, prometaphase, unaligned metaphase, metaphase, anaphase/telophase, and cytokinesis (Fig. 2 b).

Results from such mitotic counts indicate that the overexpression of cyclin E leads to the accumulation of KB cells in prometaphase (Fig. 2 c, ad cyclin E = 31% and ad control = 24% of the mitotic cells counted) and unaligned metaphase (Fig. 2 c, ad cyclin E = 20% and ad control = 13%) compared with control cells. The accumulation of cells at early stages of mitosis appears to include later stages of prometaphase up until the interval of alignment of chromosomes on the metaphase plate but not including the point of complete chromosome alignment. Consequently, the aligned metaphase population was decreased as a percentage of the entire mitotic population (adenovirus cyclin E = 13% and adenovirus control = 19%). However, once cells overexpressing cyclin E recover from the delay and proceed into anaphase, they traverse the later phases of mitosis without delay relative to controls.

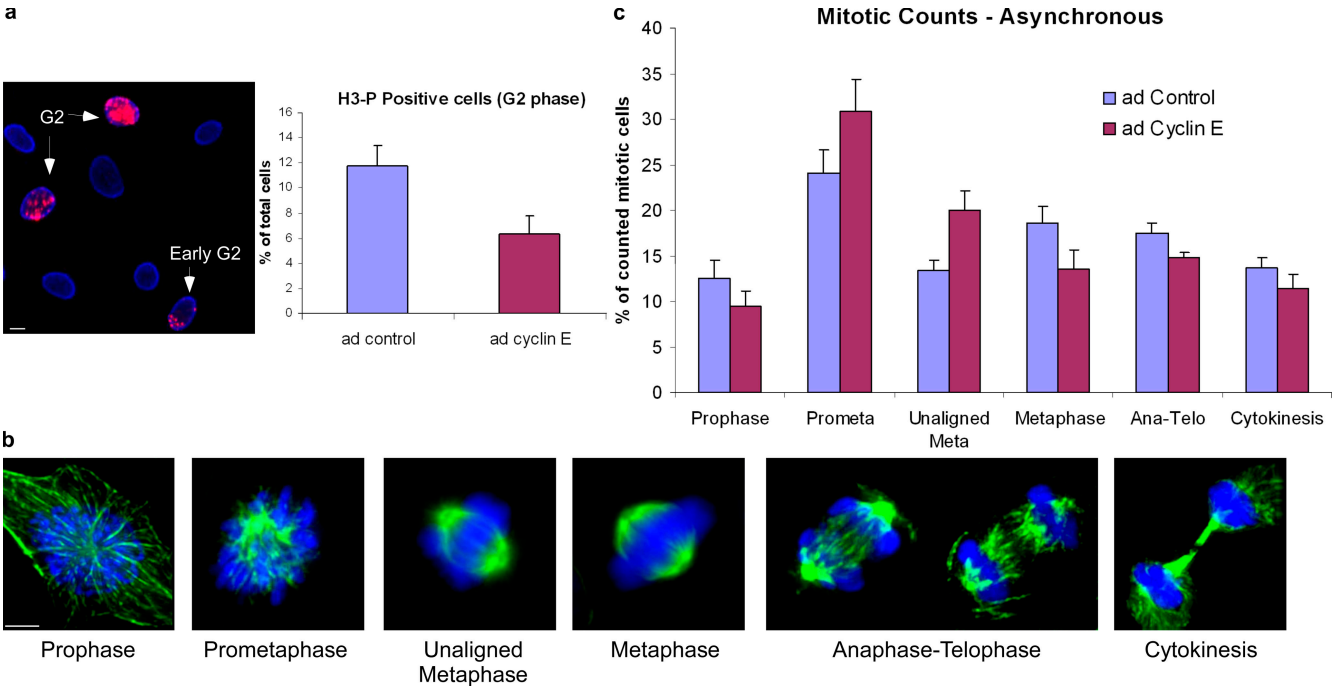

Figure 2. **Cells overexpressing cyclin E accumulate in early mitosis rather than in G2 phase.** (a) A representative immunofluorescence image of U2OS cells acquired using deconvolution microscopy showing phosphorylated histone H3 (H3-P) in red and DNA based on DAPI staining in blue. A graph showing the percentage of H3-P–positive interphase cells in an asynchronous population when transduced with either cyclin E or EV control retrovirus. Error bars represent SEM based on four experiments counting 600 cells. (b) Examples of cells in the six mitotic phases scored in this study for fixed cell mitotic counts in an asynchronous population: prophase, prometaphase, unaligned metaphase, metaphase, anaphase/telophase, and cytokinesis. DNA was detected using DAPI (blue), and microtubules were detected using antitubulin antibodies (green). (c) Graph comparing the percentages of cells in each mitotic phase out of the total of mitotic cells counted after transduction with EV control or cyclin E adenovirus. n = 300 mitotic cells counted in five experiments. Error bars represent SEM. Bars (a), 10 μm; (b) 5 μm.

An early mitotic delay is observed by live cell microscopy

For a more complete analysis of mitotic defects caused by the overexpression of cyclin E, mitotic division was observed in real time. Immortalized mammary epithelial (IME) and U2OS cells were transduced with a GFP-tagged histone H2B-expressing retrovirus to observe the dynamics of mitotic chromosomes. Cells transduced with cyclin E or control adenovirus were filmed as they progressed through mitosis.

The recordings of IME and U2OS cells provided direct real-time evidence that the overexpression of cyclin E confers an early mitotic delay. In addition, they provided insight into the dynamics of the prometaphase delay. For live cell recordings, unaligned metaphase could not be accurately determined as a result of the lack of spindle labeling. Therefore, prometaphase was scored as the time from chromosome congression toward the midzone until all chromosomes were completely aligned at the metaphase plate. Fig. 3 d shows the mean time in minutes of prometaphase, metaphase, and anaphase/telophase based on recordings of control or cyclin E adenovirus-transduced cells undergoing mitosis. Cyclin E–overexpressing cells spent on average almost twofold longer in prometaphase than controls (adenovirus cyclin E = 26–29 min and adenovirus control = 11–16 min, depending on cell type). In some abnormal mitoses characteristic of cyclin E–overexpressing cells, chromosomes oscillated near to the metaphase plate for an extended period before finally progressing into anaphase with either aligned or unaligned chromosomes. Fig. 3 a illustrates mitotic division in a control U2OS cell. Prometaphase is ~15 min, and metaphase begins at 20 min (indicated by the red asterisk in Fig. 3 a). Fig. 3 (b and c) shows mitotic divisions in cells overexpressing cyclin E with delayed and abnormal prometaphases. In the second series, a cyclin E–transduced IME cell (Fig. 3 b) shows an abnormal prometaphase (>30 min) during which chromosomes never progressed to a successful metaphase and began anaphase after 38 min despite a failure of chromosome alignment. In the third series, a cyclin E–transduced U2OS cell (Fig. 3 c; also shown in Video 1, available at http://www.jcb.org/cgi/content/full/jcb.200703202/DC1) delayed in prometaphase for almost 40 min, during which chromosomes nearly aligned at the metaphase plate but proceeded to oscillate near the plate for a prolonged period until the recording ended. Another demonstration of a cell overexpressing cyclin E expression that delays before complete metaphase alignment is shown in Video 2.

In addition to the early mitotic delays, mitotic failures were observed in which cells overexpressing cyclin E did not progress into anaphase but instead began to decondense chromosomes, resulting in a polyploid cell (Video 3, available at http://www.jcb.org/cgi/content/full/jcb.200703202/DC1). This was consistent with our previous observation of an accumulation of polyploid cells in cyclin E–overexpressing populations (Spruck et al., 1999). Indeed, flow cytometric analysis of cyclin E–overexpressing cells indicates a dose-dependent

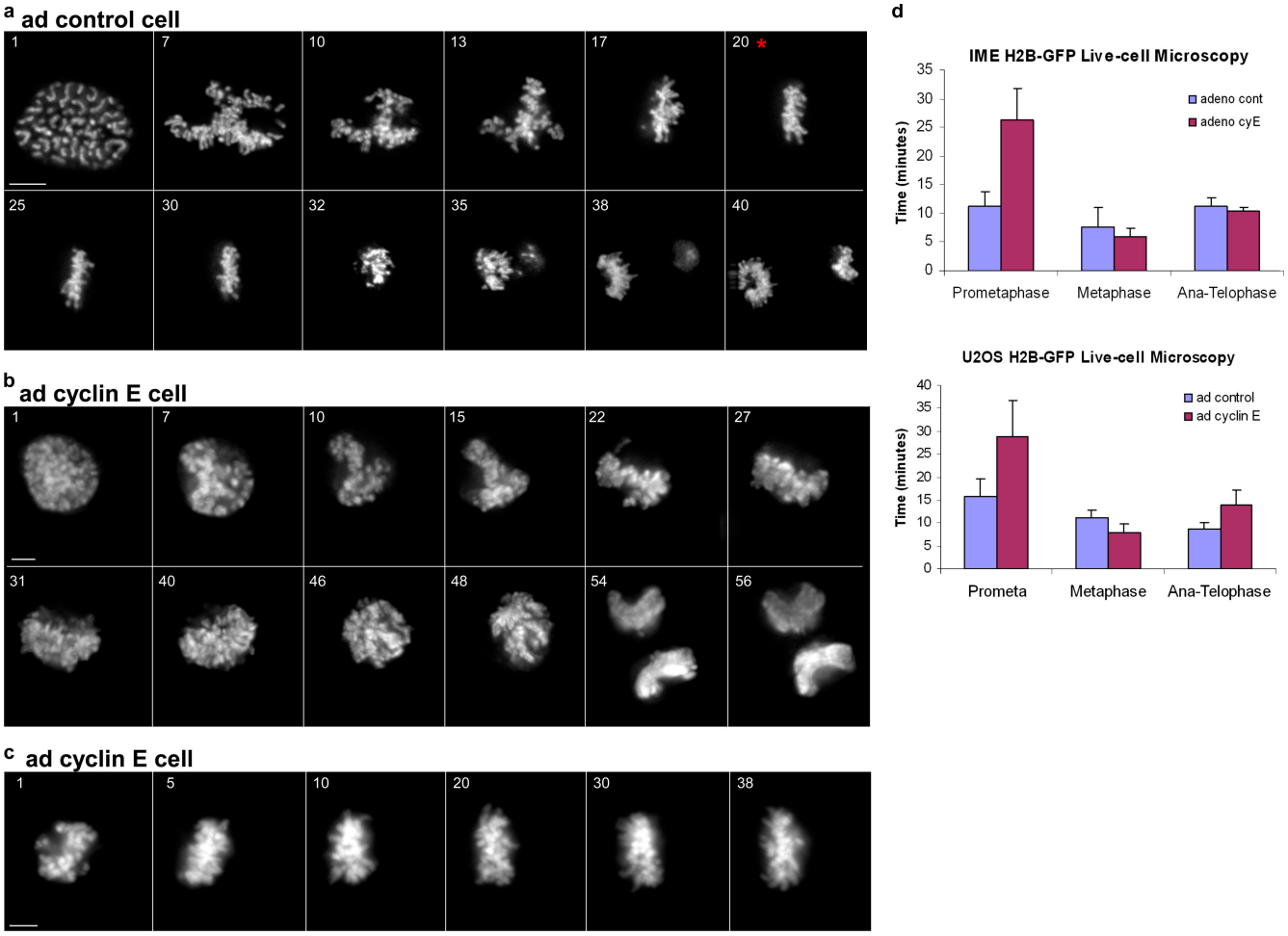

Figure 3. **Quantitation of cyclin E–mediated mitotic delay by live cell microscopy.** Live cell microscopy was performed using IME and U2OS cells expressing histone H2B-GFP for the visualization of chromosome dynamics. Differential interference contrast (not depicted) and fluorescence (GFP) images were recorded once per minute during mitosis using a deconvolution microscope. The time elapsed after recording is indicated at the top left of each frame. Select frames are shown from representative U2OS and IME videos. The red asterisk marks metaphase. (a) A control U2OS cell that begins in prophase, progresses into prometaphase, aligns all chromosomes by 20 min (the longest prometaphase recorded in control cells), and initiates chromosome segregation after 31 min. (b) An IME cell overexpressing cyclin E that begins in prophase and quickly progresses into prometaphase but never completely aligns all chromosomes. After 38 min, chromosome segregation begins despite a failed metaphase. (c) A U2OS cell overexpressing cyclin E that begins in prometaphase and continues for 40 min, during which chromosomes migrate toward the metaphase plate but never completely align (also shown in Video 2, available at http://www.jcb.org/cgi/content/full/jcb.200703202/DC1). (d) Graphs showing the mean time (in minutes) that IME and U2OS cells spend in each phase of mitosis. Error bars represent one SD. $n = 5$ recordings each of IME cells overexpressing cyclin E or controls and 7 recordings each of U20S cells overexpressing cyclin E or controls. Bars, 5 μm.

failure of mitosis at levels ≥1–2% per cell division (Fig. S2). Together, analysis of mitosis in both fixed and live cells suggests that a primary consequence of cyclin E overexpression is mitotic impairment, which, in extreme cases, can lead to mitotic failure and polyploidy.

Cyclin B1 expression is up-regulated, and degradation is delayed in metaphase as a result of cyclin E overexpression

To investigate the cause of the cyclin E–mediated mitotic delay, levels of mitotic regulatory proteins were determined. Single cell analysis of cyclin B1 expression was used to compare peak levels of cyclin B1 in early mitosis and its degradation in metaphase in cells overexpressing cyclin E and controls. KB cells were released into mitosis from a single thymidine block. Representative images of mitosis in cells transduced with either control or cyclin E adenovirus are shown in Fig. 4 a. Cyclin B1 (Fig. 4 a, green), a centromere-binding protein (Fig. 4 a, red), and DNA (Fig. 4 a, blue) were labeled, and cyclin B1 levels were measured in early prometaphase cells, unaligned metaphase cells, and metaphase cells. Cyclin B1 staining intensities of each cell were divided into low, medium, and high categories (Fig. 4 b). The overexpression of cyclin E led to elevated levels of cyclin B1 in prometaphase and unaligned metaphase. Furthermore, in metaphase, all control cells expressed low levels of cyclin B1, as expected as a result of its degradation by the mitotic ubiquitin ligase anaphase-promoting complex (APC^{Cdc20}). However, the degradation of cyclin B1 was delayed in 45% of metaphase cells with cyclin E overexpression, which continued to express medium and high levels of cyclin B1 (Fig. 4 b, metaphase). These results suggest that overexpression of cyclin E can delay the normal degradation of cyclin B1. However, cyclin B1

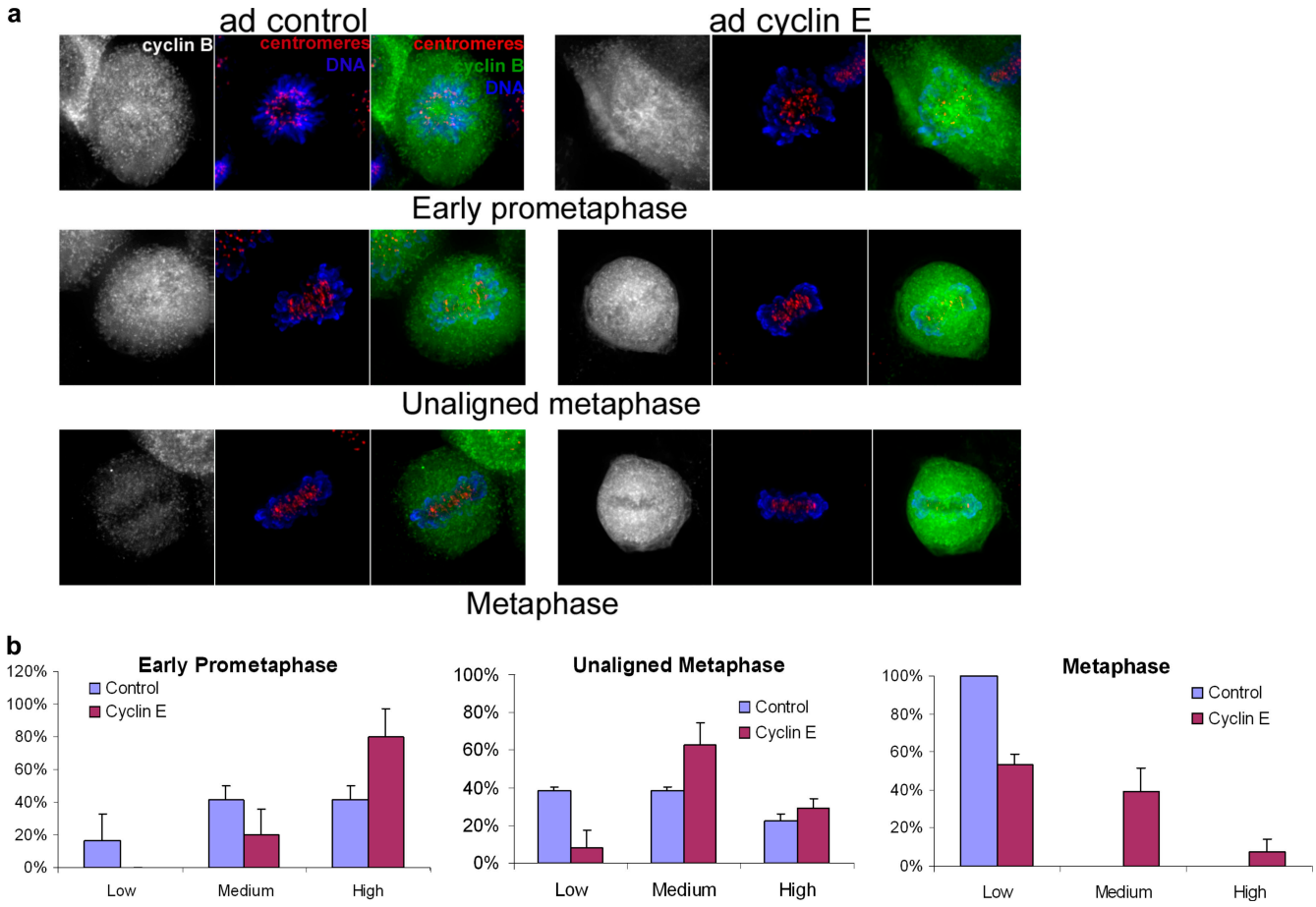

Figure 4. **Cyclin E overexpression leads to the excessive accumulation of cyclin B1 during prometaphase and a delay in cyclin B1 degradation during metaphase.** (a) Immunofluorescence images comparing KB cells transduced with either EV control adenovirus (left) or cyclin E adenovirus (right) in early prometaphase, unaligned metaphase, and metaphase. Cyclin B1, a centromere-binding protein, and DNA were stained in fixed cells, and images were acquired using a deconvolution microscope. (b) Graphs from early prometaphase, unaligned metaphase, or metaphase populations showing the percentage of EV control and cells overexpressing cyclin E with low, medium, or high cyclin B1 levels. ImageJ was used to measure mean pixel intensities of cyclin B1 in cells from 8-bit grayscale images. The area of each cell was used to account for variations in cell size. Cyclin B levels were arbitrarily divided into low, medium, and high groupings. X axis, cyclin B1 level; y axis, percentage of the total number of cells. $n = 10$ control and cyclin E–overexpressing cells each per mitotic phase. Error bars correspond to the variance based on two experiments.

degradation was not completely inhibited, as anaphase cells from both control and cyclin E–overexpressing cells contained low levels of cyclin B1 (unpublished data).

Cyclin E overexpression causes the accumulation of APC substrates up to and through mitosis

Next, protein levels of other important APC/C substrates were assessed during mitosis. For these experiments, cells were transduced with adenovirus and simultaneously arrested in a single thymidine block overnight. As adenoviral cyclin E is not expressed at substantial levels before 8 h after transduction (unpublished data), the majority of nonthymidine-blocked cells will have passed through mitosis and early G1 before cyclin E accumulation. Therefore, this protocol precludes S-phase defects conferred by cyclin E–mediated interference with prereplication complex assembly in late telophase. In addition, the single thymidine block and release protocol ensures approximately equal percentages of cells in G2/M for each time point (Fig. 5 a). In KB cells, the peak of mitosis based on microscopic observation occurs from 8 to 10 h after release from a thymidine block. Western blot analysis of protein expression up to and through mitosis in cyclin E–overexpressing and control cells revealed an accumulation of cyclin B1, Cdc20, and securin (Fig. 5, b and c). In cells overexpressing cyclin E, mitotic protein levels were elevated relative to controls at each time point up to and through the peak mitotic samples. These data indicate that defects in mitotic protein expression are not cyclin B specific but rather suggest that the APC/C ubiquitin ligase is inhibited under conditions of cyclin E overexpression, as all of the proteins exhibiting elevated expression are APC/C substrates targeted for ubiquitin-mediated proteolysis.

To determine whether the observed protein accumulations were caused by decreased degradation, we examined protein stability by carrying out cycloheximide chase experiments under conditions of cyclin E overexpression. Cells transduced with cyclin E or control adenovirus and arrested using a single thymidine block were then released for 4 h. Cycloheximide was added to terminate protein synthesis, and samples were collected, as indicated, for Western blot analysis (Fig. 5, d and e).

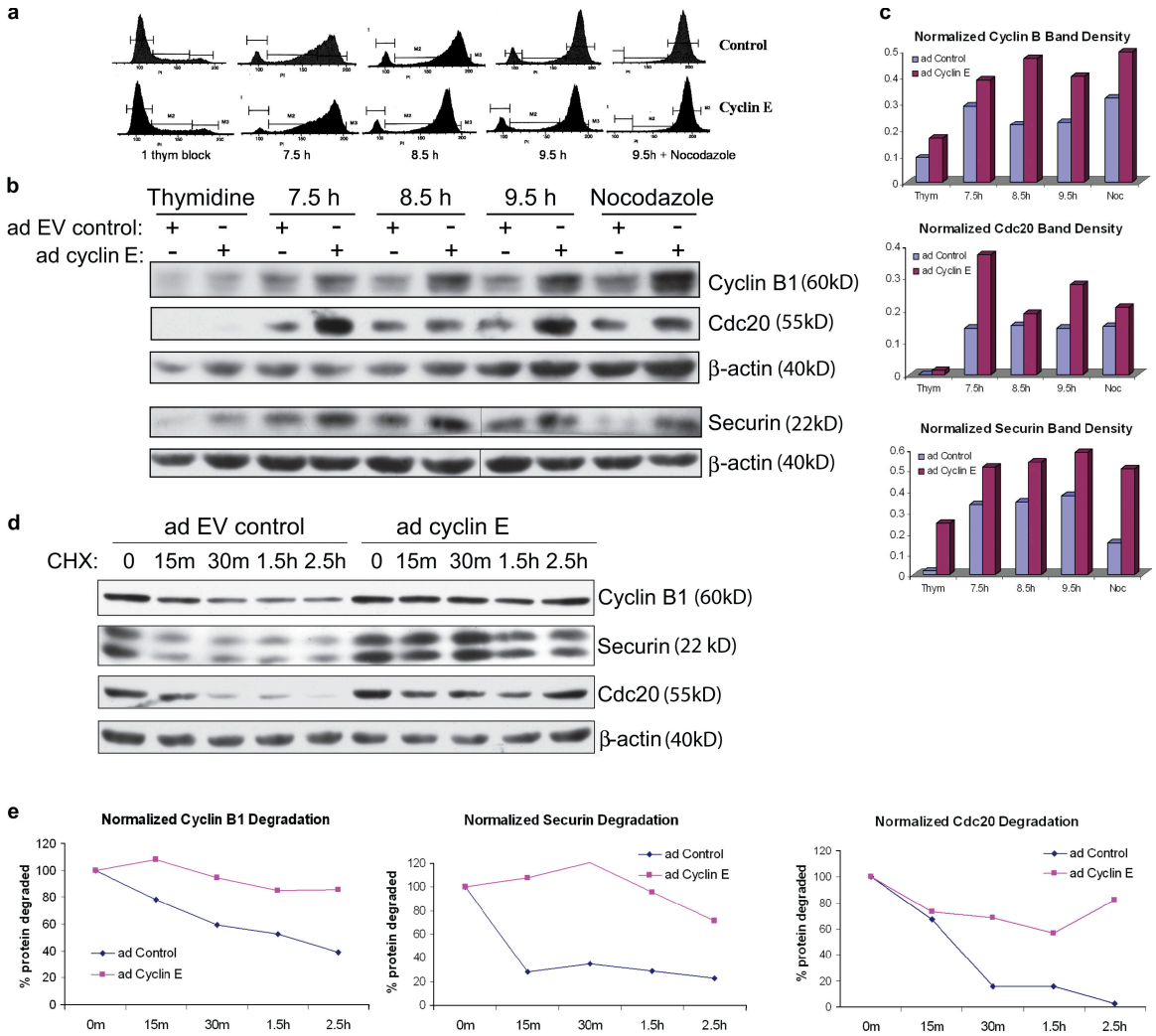

Figure 5. **Cyclin E overexpression causes the accumulation of APC/C substrates up to and through mitosis as a result of increased protein stability.** (a) Representative FACS profiles (propidium iodide staining) from EV control and cyclin E adenovirus–transduced KB cells collected at specific times after release from a thymidine block. (b) Representative Western blot analyses showing the elevated expression of APC/C substrates cyclin B, Cdc20, and securin in cyclin E–overexpressing cells compared with control cells. β-actin is used as a loading control in both experiments. Dividing lines represent splicing of an empty lane from the blot. (c) Band densities from panel b quantified and normalized to actin. (d) Western blot analysis of a cycloheximide (CHX) chase experiment showing the stabilization of APC/C substrates under conditions of cyclin E overexpression. Degradation of cyclin B, securin, and Cdc20 was assayed after thymidine synchronization and a 4-h release into late S/G2 phase. Cycloheximide was added at 0 min, and samples were collected at 0 min, 15 min, 30 min, 1.5 h, and 2.5 h after cycloheximide addition. (e) Quantitation of the cycloheximide chase experiment in panel d. Band intensities were normalized to actin.

As can be seen, cyclin B1, securin, and Cdc20 were degraded much more rapidly in control cells compared with cells overexpressing cyclin E, suggesting that the cyclin E–mediated accumulation of key mitotic regulatory proteins occurs by decreasing their rate of ubiquitin-mediated proteolysis.

Overexpressed cyclin E–Cdk2 binds and phosphorylates Cdh1

The data presented up to this point suggest that elevated cyclin E–Cdk2 inhibits the APC/C. APC/C activity requires one of two activating regulatory subunits, Cdc20 or Cdh1 (Visintin et al., 1997; Kramer et al., 2000). Cdc20 is thought to activate the APC/C during mitosis, whereas Cdh1 is the activating subunit from mitotic exit to the G1/S boundary (Fang et al., 1998; Jaspersen et al., 1999; Lukas et al., 1999; Blanco et al., 2000; Kramer et al., 2000; Sorensen et al., 2000). Because Cdc20 itself was found to accumulate in response to cyclin E overexpression, it was unlikely to be the relevant target of cyclin E–Cdk2. On the other hand, whereas Cdh1 is inactivated by phosphorylation, it is thought to already be inactive during early mitosis as a result of the phosphorylation by cyclin A–Cdk2 (Lukas et al., 1999; Sorensen et al., 2001). However, recent studies have suggested that Cdh1 does contribute to early mitotic APC/C activation (Jeganathan et al., 2005, 2006), raising the possibility that it is the target of cyclin E overexpression. Furthermore, although under normal circumstances, it was shown that cyclin E–Cdk2 does not contribute substantially to Cdh1 phosphorylation and inactivation (Brandeis and Hunt, 1996; Lukas et al., 1999; Sorensen et al., 2001), overexpressed cyclin E might be able to interact with and phosphorylate Cdh1.

We first determined whether cyclin E–Cdk2 could bind directly to Cdh1 because protein kinases often form stable complexes with substrates. Cyclin A binding to Cdh1 has previously been described and was used as a positive control (Lukas et al., 1999; Sorensen et al., 2001). Three expression plasmids coding for N-terminally myc-tagged WT or mutants $Cdh1^{RVL\text{-}AAA}$ and $Cdh1^{4A}$ were used to characterize the binding of cyclin E and cyclin A to Cdh1 (Sorensen et al., 2001). $Cdh1^{RVL\text{-}AAA}$ is mutated in the WD-40 repeat domain at the RVL motif, which has been shown to be necessary for cyclin A binding, and $Cdh1^{4A}$ is mutated at four phosphorylation sites shown to be targeted by cyclin A–Cdk2 that are essential for Cdh1 inhibition. Expression plasmids for cyclin E or cyclin A were cotransfected with expression plasmids encoding $Cdh1^{WT}$, $Cdh1^{AAA}$, $Cdh1^{4A}$, or an empty vector into 293T cells. Cdh1 was immunoprecipitated from cell lysates using anti-myc antibody. The immunoprecipitation data show that exogenous cyclin E binds efficiently to $Cdh1^{WT}$ as does the positive control, cyclin A (Fig. 6 a). In addition, weak binding is detectable between exogenous cyclin A and both Cdh1 mutants. Exogenous cyclin E also bound both WT and, to a lesser degree, both mutant Cdh1 mutants. However, no binding was observed at endogenous levels of cyclin E (shown as a band with lower mobility than exogenous cyclin E), which is consistent with previous results (Sorensen et al., 2001).

To determine whether Cdh1 is a substrate of cyclin E–Cdk2, in vitro phosphorylation assays were performed. GST-Cdh1 (Sorensen et al., 2001) and GST alone were purified from *Escherichia coli*. In vitro kinase assays were performed using

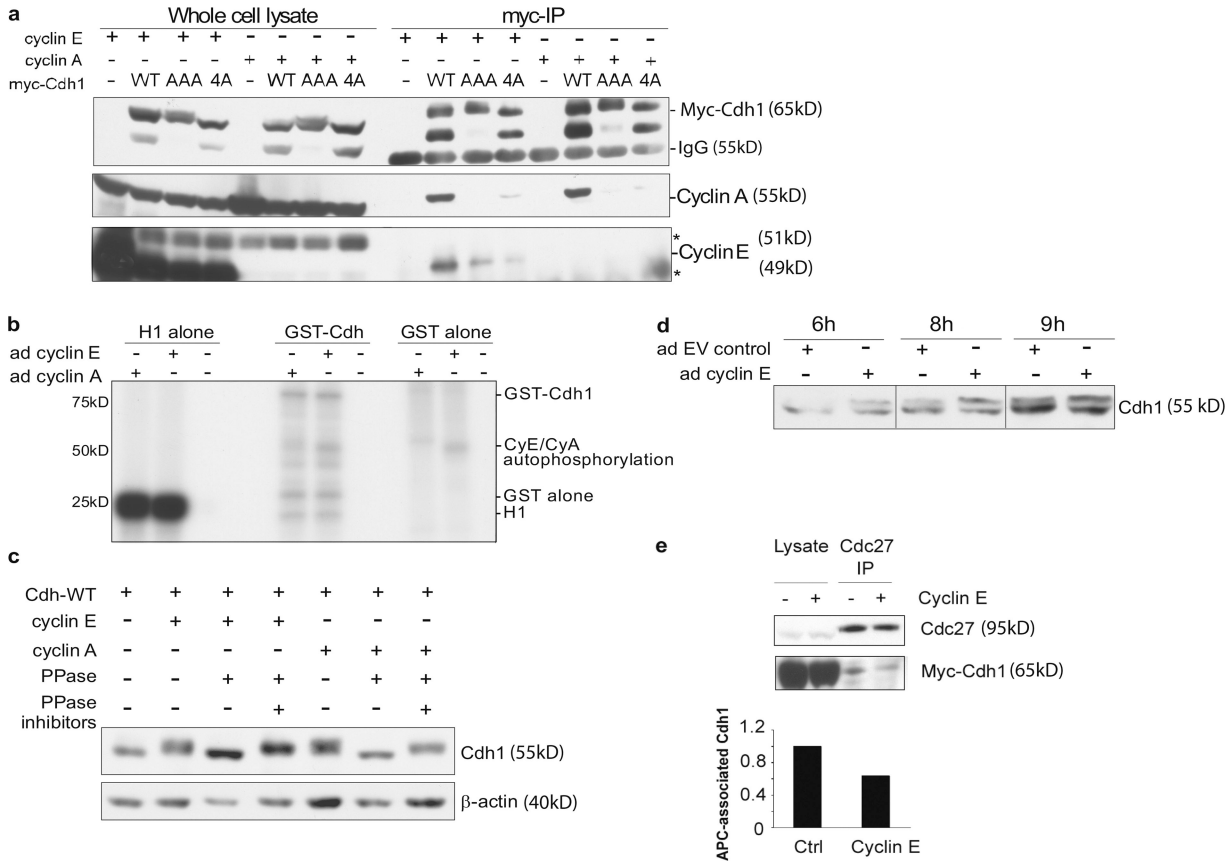

Figure 6. **Cyclin E and cyclin A can bind and phosphorylate the APC-activating subunit Cdh1, leading to reduced association with the APC.** (a) Immunoprecipitation assay using the empty vector or one of three myc-tagged Cdh1 constructs: WT (wild-type), AAA (an RxL motif cyclin-binding mutant), or 4A (a phosphorylation site mutant). Cdh1 and cyclin E or cyclin A expression plasmids were transiently transfected into 293T cells. Cell lysates were immunoprecipitated with anti-myc antibody, separated by SDS-PAGE, and detected by Western blotting. Both exogenous and endogenous cyclin A are detected using anti–cyclin A. Endogenous and exogenous cyclin E are detected using an anti–cyclin E antibody (endogenous cyclin E is observed migrating more slowly than exogenous; both are marked with asterisks). (b) In vitro kinase assay with GST-Cdh1 purified from *E. coli*. Purified cyclin E–Cdk2, cyclin A–Cdk2, or buffer were incubated with γ-[^{32}P]ATP and either histone H1 (first three lanes), GST-Cdh1 (middle three lanes), or GST alone (last three lanes). (c) Cdh^{WT} exhibits reduced mobility upon the cotransfection of cyclin E or cyclin A as a result of increased phosphorylation. Transfection of 293T cells was performed as described in panel a. Cell lysates were incubated with λ-phosphatase in the presence or absence of phosphatase inhibitors as indicated. Lysates were separated by SDS-PAGE and immunoblotted using anti-Cdh1 antibody for detection. β-Actin serves as a loading control. (d) Western blot showing the phosphorylation of endogenous Cdh1 in KB cells transduced with adenoviral cyclin E. Cells were transduced with EV control or cyclin E adenovirus, which was arrested using a single thymidine block, and released. Samples were collected as cells progressed into and through mitosis and were analyzed for Cdh1 migration by SDS-PAGE followed by Western blotting and detection using anti-Cdh1 antibody. Slower migrating band represents hyperphosphorylated Cdh1 based on the experiment shown in panel c. Lines indicate where irrelevant lanes were spliced out. (e) Cdc27 immunoprecipitation quantitating APC-associated Cdh1 in synchronized S/G2 cells. Cells were transfected with a plasmid expressing myc-tagged Cdh1 and were transduced with cyclin E–expressing or control adenovirus. 4 h after release from a thymidine block, lysates were prepared and immunoprecipitated using Cdc27 antibody. Lysates and immunoprecipitates were separated by SDS-PAGE followed by Western blotting using Cdc27 and Cdh1 antibody. The graph represents the Cdh1 band density normalized to the Cdc27 band density, where the control ratio is arbitrarily set to 1.0.

cyclin E– and cyclin A–Cdk2 purified from baculovirus-transduced insect cells on histone H1, GST, and GST-Cdh1 as substrates (Fig. 6 b). Robust phosphorylation of histone H1 by cyclin E– and cyclin A–Cdk2 confirmed that both kinase complexes were active. GST alone (~28 kD) was not phosphorylated by either cyclin–Cdk2 complex. However, purified GST-Cdh1 (75 kD) as well as several degradation products were phosphorylated by both cyclin E– and cyclin A–Cdk2.

Phosphorylation of Cdh1 was also confirmed in cell culture. In Fig. 6 a, reduced mobility was shown for $Cdh1^{WT}$ and $Cdh1^{RVL\text{-}AAA}$ when coexpressed with either cyclin E or cyclin A. To ensure that the reduced mobility was a result of the phosphorylation of Cdh1, parallel samples using $Cdh1^{WT}$ were treated with λ-phosphatase to dephosphorylate Cdh1 before analysis (Fig. 6 c). Cdh1 exhibited reduced mobility upon the cotransfection of either cyclin E or cyclin A, which was reversed with phosphatase treatment, but not when phosphatase inhibitors were present, indicating that ectopically expressed Cdh1 can be phosphorylated by either cyclin E– or cyclin A–Cdk2.

Next, we assessed the ability of cyclin E–Cdk2 to phosphorylate endogenous Cdh1 under conditions in which the cyclin E–mediated accumulation of mitotic APC/C substrates was observed (as in Fig. 5). Samples were collected up to and through mitosis after a thymidine block and release (Fig. 6 d). Overexpression of cyclin E reduced the mobility of endogenous Cdh1 (Fig. 6 d), which is consistent with cyclin E–Cdk2 contributing substantially to the phosphorylation and inactivation of Cdh1 under these conditions. To determine whether the phosphorylation of Cdh1 by cyclin E–Cdk2 under these conditions affected the association of Cdh1 with APC, cells were transfected with a plasmid expressing myc-Cdh1 and were transduced with cyclin E–expressing or control adenovirus. APC immunoprecipitates (using Cdc27 antibody) were then prepared 4h after release from a thymidine block. Cdh1 association with the APC was reduced to ~60% of control values as a consequence of cyclin E overexpression (Fig. 6 e).

Cyclin E–Cdk2 inhibits the APC^{Cdh1}-dependent ubiquitylation of cyclin B1 in vitro

To assess the effects of cyclin E–Cdk2 on the activity of APC^{Cdh1} directly, in vitro ubiquitylation assays were performed (Fig. 7). Cdh1 was phosphorylated in vitro before addition to the ubiquitylation reaction. APC^{Cdh1} activity was determined by the conversion of unmodified cyclin B1 to multiubiquitylated cyclin B1 derivatives.

Cyclin B1 was efficiently ubiquitylated when Cdh1 was added to the reaction in the absence of cyclin E–Cdk2 (Fig. 7 a). Upon the addition of purified cyclin E–Cdk2, the ubiquitylation of cyclin B1 was dramatically reduced, which is consistent with the phosphorylation-dependent inhibition of Cdh1 (Fig. 7 a; and quantified in b). The addition of purvalanol, a Cdk inhibitor, partially reversed cyclin E–mediated inhibition. These data suggest that cyclin E–Cdk2 inhibits Cdh1 via phosphorylation. Furthermore, a phosphorylation site mutant of Cdh1, where all possible Cdk sites were mutated to alanines, was

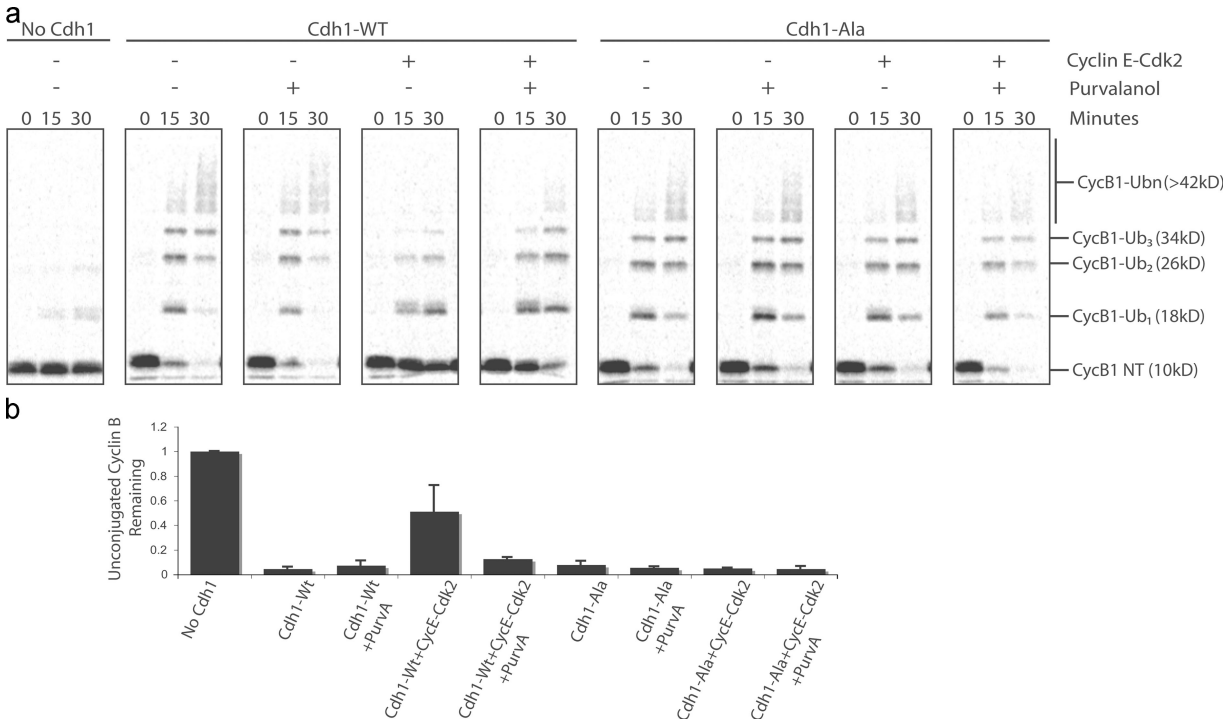

Figure 7. **Cyclin E–Cdk2 inhibits APC^{Cdh1} ubiquitin ligase activity in vitro through a kinase-dependent mechanism.** (a) In vitro ubiquitylation was used to assess inhibition of the APC^{Cdh1} by cyclin E–Cdk2. Autoradiography was used to visualize both the unmodified and ubiquitin-conjugated ^{35}S-labeled N-terminal fragment of cyclin B1. The addition of cyclin E–Cdk2 and/or the Cdk inhibitor purvalanol A to the various reactions is indicated. Reactions were performed in parallel with WT Cdh1 (Cdh1-WT) and a Cdk phosphorylation site mutant (Cdh1-Ala). (b) Quantitation of unmodified cyclin B1 remaining in the reactions shown in panel a. Error bars represent the variance of the mean from two independent experiments.

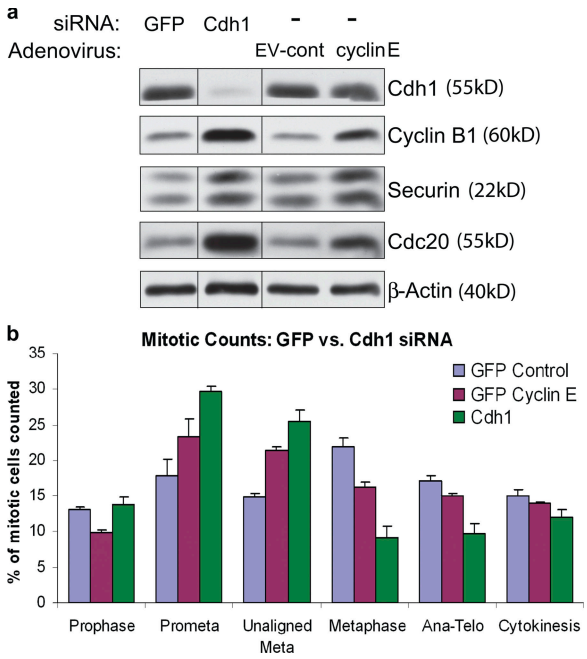

Figure 8. **Reducing Cdh1 by RNAi mimics cyclin E overexpression, resulting in mitotic protein accumulation and early mitotic delay.** (a) Western blot comparing the accumulation of cyclin B1, securin, and Cdc20 in cells subjected to partial silencing of Cdh1 using siRNA or overexpressing cyclin E. Asynchronous populations were collected and analyzed by immunoblotting. Dividing lines indicate where the gel was spliced to remove irrelevant lanes. (b) Mitotic counts of cells subjected to Cdh1-specific RNAi. Cells were transfected with Cdh1-specific siRNA or transduced with EV control or cyclin E adenovirus followed by transfection with GFP-specific siRNA. $n = 300$ cells per sample. Error bars correspond to the SEM based on three experiments.

completely resistant to cyclin E–Cdk2-mediated inhibition (Fig. 7 a; and quantified in b). These data confirm that cyclin E–Cdk2 can inactivate APC^{Cdh1} through the inhibitory phosphorylation of Cdh1.

Reduction of Cdh1 levels results in mitotic protein accumulation and mitotic delay similar to the overexpression of cyclin E

If cyclin E–Cdk2 inhibits APC^{Cdh1} in vivo, reducing cellular levels of Cdh1 should mimic the phenotype associated with the overexpression of cyclin E. Using Cdh1-specific siRNA, the effects of Cdh1 reduction were compared with those associated with cyclin E overexpression. A strong knockdown of Cdh1 protein (using 20 nM of Cdh1-specific siRNA) inhibited cell proliferation, which had previously been reported (Sorensen et al., 2001; Gimenez-Abian et al., 2005b). To only partially ablate Cdh1, the time of incubation and the concentration of Cdh1-specific siRNA were reduced. The accumulation of cyclin B1, securin, and Cdc20 in cells targeted by Cdh1-specific siRNA was compared with that in cells transduced with cyclin E or control adenovirus (Fig. 8 a). A comparable up-regulation of cyclin B1, securin, and Cdc20 protein occurs as a result of both Cdh1 reduction and cyclin E overexpression.

We next determined the effects of reducing Cdh1 on mitotic progression. Fixed cells were scored as previously discussed (see section Cyclin E overexpression leads to an early mitotic delay) in asynchronous populations after the transduction of EV control or cyclin E adenovirus for 24 h and incubation with Cdh1- or GFP-specific siRNA for an additional 24 h (Fig. 8 b). As shown previously, cyclin E overexpression caused an accumulation in early mitosis before metaphase. This same trend, but with a more pronounced effect, was observed in cells partially silenced for Cdh1 (Fig. 8 b). These data confirm that Cdh1 has a role in the regulation of progression through early mitosis and that cyclin E–mediated inhibition of Cdh1 could, in principle, account for the impairment of early mitotic events.

Reducing the levels of APC^{Cdh1} substrates cyclin B1 and securin in cells overexpressing cyclin E allows progression through mitosis without delay

Based on the aforementioned data, the direct reduction of Cdh1 or overexpression of cyclin E leads to the accumulation of mitotic APC/C substrates and delay in progression through early mitosis. However, whether the mitotic delay is caused by the accumulation of APC/C substrates and, if so, which APC/C substrates contribute to the mitotic delay remained to be determined. Based on our observations, it appeared that most chromosomes become bioriented but delay in aligning at the metaphase plate and progressing into anaphase. This phenotype is consistent with a defect in sister chromatid separation possibly caused by elevated levels of cyclin B1 and securin as cells progress into and through mitosis. Degradation of securin and cyclin B1 is needed to activate separase and thereby promote the cleavage of cohesin (Gorr et al., 2005; Ji et al., 2005), which is required for separation of the sister chromatids at anaphase, allowing the poleward migration of chromosomes (Uhlmann et al., 1999, 2000; Hauf et al., 2001; Gimenez-Abian et al., 2005a). Therefore, we tested whether slightly reducing securin and cyclin B1 expression in cells overexpressing cyclin E could override the cyclin E–induced delay of early mitosis.

Cells were transduced with EV control or cyclin E adenovirus for 24 h and transfected with low concentrations of siRNA (10 pM) targeting securin and/or cyclin B1 or GFP for an additional 24 h. Expression of cyclin B1 and securin in cells released into mitosis from a thymidine block was compared by Western blot analysis (Fig. 9 a). Cells transduced with cyclin E adenovirus and transfected with cyclin B1– and securin-specific siRNA resulted in levels of cyclin B1 and securin comparable with those found in control cells, whereas cells transfected with control GFP-specific siRNA continued to exhibit elevated levels of cyclin B1 and securin. As expected, Cdc20 levels were not affected by siRNA targeting cyclin B1 and securin.

Mitotic progression was assessed in cells with reduced levels of securin and cyclin B1, securin alone, or cyclin B1 alone mediated by siRNA transfection (Fig. 9 b). Reducing both cyclin B1 and securin eliminated the delays in prometaphase and unaligned metaphase along with the resulting decrease in the percentage of metaphase cells mediated by cyclin E overexpression. However, reducing securin or cyclin B1 alone did not completely eliminate the prometaphase or unaligned metaphase delay associated with cyclin E overexpression. Therefore, the

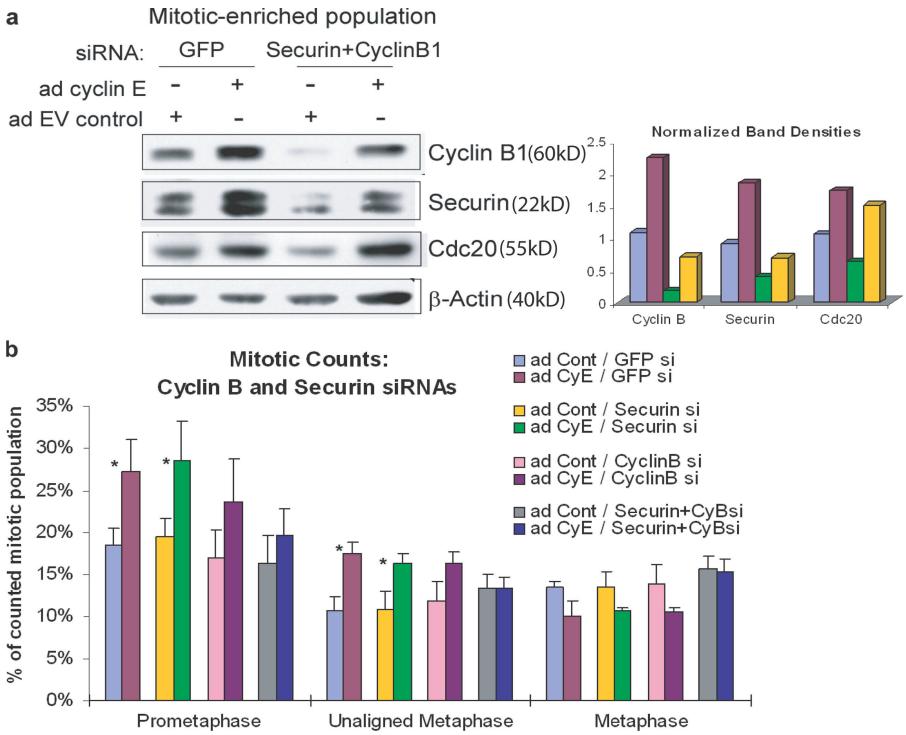

Figure 9. **Reducing the accumulation of APC^{Cdh1} substrates cyclin B1 and securin in cells overexpressing cyclin E restores normal progression through mitosis.** (a) Elevation of mitotic regulatory proteins cyclin B1 and securin in mitotically enriched KB cells overexpressing cyclin E can be reversed using low concentrations of sequence-specific siRNA. Cells were subjected to a single thymidine block and harvested 8 h after release. Cyclin B1 and securin levels were reduced by transfection with corresponding siRNAs. Band densities normalized to actin are shown beside the Western blot. (b) Mitotic progression in cells overexpressing cyclin E is no longer delayed if the hyperaccumulation of both cyclin B1 and securin are prevented by sequence-specific RNAi. Cells were transduced with cyclin E or EV control adenovirus followed by transfection with sequence-specific siRNA as indicated and were processed for immunofluorescence as described in Materials and methods. Mitotic counts of fixed KB cells were performed as described in Materials and methods. The graph compares percentages of prometaphase, unaligned metaphase, and metaphase out of the total mitotic population counted from cells treated with GFP siRNA, individual targeting of securin or cyclin B1, and simultaneous targeting of cyclin B1 and securin. Error bars represent the SEM based on three experiments. Asterisks indicate comparisons in which the difference reaches a ≥90% confidence level (*, $P \leq 0.1$).

depletion of securin or cyclin B1 alone is not sufficient to alleviate the mitotic inhibitory effects of cyclin E overexpression and suggests that stabilization of both proteins contributes to cyclin E–mediated mitotic delay.

Discussion

Inhibition of APC^{Cdh1} affects progression through early stages of mitosis

Although Cdh1 can activate both mitotic and interphase APC/C, models of cell cycle regulation have proposed that the ubiquitin ligase ACP^{Cdh1} is maintained in an inactive state from the G1/S boundary until mitotic exit as a result of phosphorylation by Cdks active during this interval (Zachariae et al., 1998; Jaspersen et al., 1999; Lukas et al., 1999; Blanco et al., 2000; Kramer et al., 2000; Sorensen et al., 2001). Although there is evidence that cyclin E–Cdk2 is primarily responsible for the accumulation of G2/M cyclins and Cdh1 phosphorylation in *Drosophila melanogaster* (Knoblich et al., 1994; Sigrist and Lehner, 1997), in mammalian cells, it was shown that cyclin A–Cdk2 specifically phosphorylates Cdh1 on a number sites and that this phosphorylation prevents association with the APC/C core (Sigrist and Lehner, 1997; Lukas et al., 1999; Sorensen et al., 2001). Because cyclin A–Cdk2 becomes active at the G1/S transition and persists until early mitosis, it has been assumed that Cdh1 does not contribute to APC/C ubiquitin ligase activity during this interval and that only an alternative APC/C cofactor, Cdc20, carries out mitotic functions. However, a recent study suggests that APC^{Cdh1} does have a role in the ubiquitylation of securin during early mitosis in that mice carrying mutations that misregulate Cdh1 nuclear transport exhibit mitotic defects (Jeganathan et al., 2005). Consistent with this finding, in the present study, we show that APC^{Cdh1} activity must contribute to the regulation of mitotic proteins up to and through early mitosis. Specifically, the partial silencing of Cdh1 by RNAi led to a hyperaccumulation of APC substrates and impaired progression through early phases of mitosis. Therefore, APC^{Cdh1} must retain residual activity before mitosis even in the presence of cyclin A–Cdk2. This conclusion, along with the observed ability of cyclin E–Cdk2 to phosphorylate Cdh1 in vivo and inhibit APC^{Cdh1} in vitro, is consistent with a model in which cyclin E–mediated effects on mitosis are caused by the inhibition of residual APC^{Cdh1} activity.

This proposal is seemingly at odds with previous reports that cyclin E–Cdk2 does not bind to Cdh1 or contribute to its phosphorylation in mammalian cells (Lukas et al., 1999; Sorensen et al., 2001). Indeed, we could not detect an association between endogenous cyclin E and Cdh1. However, when cyclin E was overexpressed by transfection, the association of cyclin E with Cdh1 and the cyclin E–mediated hyperphosphorylation of Cdh1 were readily detectable. These data suggest that when normally expressed at the G1/S boundary, cyclin E is unlikely to have a major impact on Cdh1 regulation. However, overexpressed cyclin E, either in the experimental contexts reported here or in the course of tumorigenesis, can influence Cdh1 activity in a manner that has functional consequences. Whether the temporal deregulation of cyclin E expression, simply the deregulation of cyclin E levels, or both allows cyclin E to have an impact on Cdh1 activity remains to be determined.

APC^{Cdh1} targets relevant to the cyclin E–mediated impairment of mitosis

Overexpression of cyclin E causes cells to delay in mitosis before anaphase. This phenotype could be explained by a cyclin E–mediated failure to activate the mitotic protease separase. Indeed, it has been reported that one defect caused by the RNAi-mediated depletion of separase is a prometaphase delay similar to that reported here in the context of cyclin E overexpression (Gimenez-Abian et al., 2005a). In addition, the depletion of separase induces polyploidy (Waizenegger et al., 2002). Separase specifically cleaves the cohesin subunit Scc1, resulting in a loss of centromeric sister chromatid cohesion in mammalian cells, potentiating anaphase (Uhlmann et al., 1999, 2000; Waizenegger et al., 2000; Hauf et al., 2001). The primary mode of separase regulation is through the binding of the separase inhibitor securin (Cohen-Fix et al., 1996; Zou et al., 1999). Securin ubiquitylation by the APC/C targeting it for proteasomal degradation during the early phases of mitosis is thought to constitute the principal mitotic regulatory role of the APC/C. However, the role of securin ubiquitylation during early mitosis has been attributed to the APC/C cofactor Cdc20 rather than Cdh1, as the latter cofactor has been assumed to be inactive during this interval (Visintin et al., 1997; Zachariae et al., 1998; Jaspersen et al., 1999; Salah and Nasmyth, 2000). Indeed, in yeast, the inactivation of Cdc20 leads to metaphase arrest, whereas the inactivation of Cdh1 has no obvious effects on early stages of mitosis (Sigrist et al., 1995; Cohen-Fix et al., 1996; Kramer et al., 2000).

Nevertheless, we show that in mammalian cells, partial silencing of Cdh1 by RNAi leads to the accumulation of securin and an early mitotic delay, and it has been reported that mammalian APC^{Cdh1} shares the capacity to target securin with APC^{Cdc20} (Zur and Brandeis, 2001). Therefore, it was reasonable to consider securin as the relevant anaphase inhibitory target stabilized by the cyclin E–mediated inhibition of Cdh1. However, when securin expression was adjusted by partial RNAi-mediated silencing so that cyclin E overexpression restored securin to normal levels, early mitotic delay was not abrogated. Recent studies have suggested that cyclin B1–Cdk1 also inhibits separase, raising the possibility that the abnormal accumulation of cyclin B1 during early mitosis may also contribute to cyclin E–mediated mitotic delay (Gorr et al., 2005; Ji et al., 2005). However, as with securin, RNAi- mediated restoration of cyclin B1 levels alone was not sufficient to completely abrogate mitotic delay. Only when the simultaneous restoration of both securin and cyclin B1 was performed were the mitotic effects of cyclin E overexpression neutralized. The contribution of two distinct and possibly synergistic mitotic inhibitors explains why seemingly modest elevation of levels of these proteins has a profound effect on progression through mitosis.

The nature of cyclin E–mediated mitotic delay

Based on observations made from fixed cells, the overexpression of cyclin E causes an accumulation of cells either in a prometaphase-like state or a state in which chromosomes are almost but not completely aligned on the metaphase plate. However, this categorization was a formalism. Because these are static observations, we cannot describe the sequence of events in real time that led to the accumulation of these cell types. It is possible that both of these phenotypes reflect the same population resulting from an inability to lose sister chromatid cohesion. Normally, centromeric cohesion is lost when bioriented chromosomes are aligned at metaphase. However, the inability to lose cohesion in a timely manner may promote an unusually dynamic situation in which chromosomes under tension cyclically move toward and away from the metaphase plate, potentially accounting for both of the observed populations that accumulate as a result of cyclin E overexpression. Indeed, in time-lapse series of such cells, chromosomes appeared to be unusually dynamic, undergoing substantial oscillatory movements for long periods of time. However, because spindles and centromeres were not visible under these circumstances, it was not possible to evaluate the attachment or tension status of chromosomes. The observation that mitotic chromosomes in cells overexpressing cyclin E appear hypercondensed (unpublished data) is also consistent with a prolonged prometaphase or metaphase caused by the inability to lose cohesion in a timely fashion (Waizenegger et al., 2002; Gimenez-Abian et al., 2005a).

Materials and methods

Cell culture and modeling cyclin E overexpression

Immortalized human fibroblasts and IME cells, two cell lines immortalized by stable transduction with a pBABEpuro retrovirus expressing the human telomerase reverse transcriptase gene (gift from J. Shay, The University of Texas Southwestern Medical Center, Dallas, TX), were used in initial experiments for chromosome painting, flow cytometry, and live cell microscopy analysis. U2OS cells, an osteosarcoma cell line, were used for immunofluorescence and live cell microscopy experiments. KB cells, a human nasopharyngeal epidermoid carcinoma, and breast cancer–derived cell lines MDA-MB-157, -436, and -468 (American Type Culture Collection) were used for immunofluorescence microscopy and biochemical experiments. IME cells were cultured in MCDB media (Invitrogen) and supplemented with 1% FCS, holotransferrin, EGF, bovine pituitary extract, insulin, L-glutamine, 100 U/ml penicillin, and 1.0 mg/ml streptomycin. All other cells were grown in DME (Invitrogen) supplemented with 10% FCS or 20% normal calf serum and 100 U/ml penicillin, 1.0 mg/ml streptomycin, and L-glutamine.

Recombinant retroviruses expressing a hyperstable form of cyclin E (T380A) or a control empty vector were prepared using the 293T-derived packaging cell line Phoenix-Ampho and the pBABE retroviral plasmid vector (Morgenstern and Land, 1990) containing a hygromycin resistance marker for the selection of long-term stable expression mediated by the constitutive retrovirus long terminal repeat promoter. Viral preparation steps are listed as follows: Phoenix-Ampho cells were transfected overnight by calcium phosphate precipitation; 24 h after transfection, medium was changed; 48 h after transfection, virus-containing medium was harvested; and 0.2 μm was filtered and frozen in aliquots for future use. Viral infection steps are listed as follows: frozen viral aliquots were thawed at RT, and retrovirus was added to cells with an equal amount of medium (10% FCS) for 24 h, after which fresh media was added. Cells carrying the retrovirus construct were selected after 48 h using 200 ng/ml hygromycin.

Recombinant adenovirus expressing WT cyclin E or a control empty vector under the constitutive cytomegalovirus promoter were purified by CsCl ultracentrifugation. Cells were transduced with $\sim$1,000 virus particles/cell (comparable with the levels used in Ekholm-Reed et al., 2004a) in a low volume of medium with 0% serum for 2 h, and then additional medium plus 10% FCS was added for 24 h. Cyclin E expression in IME, U2OS, and KB cells was assayed by Western blotting and immunofluorescence microscopy.

The histone H2B-GFP retrovirus was constructed from an H2B-GFP expression plasmid (BOS H2BGFP-N1; a gift from K. Sullivan, National University of Ireland, Galway, Ireland; Kanda et al., 1998). H2B-GFP was

cut and ligated into a pBabe backbone containing a neomycin resistance marker for selection. Viral preparation and transduction were performed as for the cyclin E retrovirus.

SDS-PAGE electrophoresis and Western blotting analysis

Lysates were extracted in cold lysis buffer (50 mM Tris, 150 mM NaCL, 1 mM EDTA, 1% Triton X-100 detergent, and phosphatase/protease inhibitors), sonicated, and cleared for 10 min at 10,000 *g* at 4°C, and protein concentrations were determined using a Bradford solution (Bio-Rad Laboratories) read at 595 nM. For Western blotting analysis, samples were separated by SDS-PAGE and transferred onto Immobilon P membranes (Millipore). Filters were then blocked for 1 h at room temperature in blocking buffer (5% nonfat milk in 1× TBS plus 0.1% Triton X-100 [TBS-T = 10 mM Tris, 500 mM NaCl, and 0.1% Triton X-100, pH 8]). Primary antibody was added in blocking buffer overnight at 4°C. HRP-conjugated secondary antibodies (1:5,000) diluted in blocking buffer were incubated with the membrane for 1 h at RT. Primary antibodies used were anti–cyclin E monoclonal antibody (HE12; Santa Cruz Biotechnology, Inc.) at 1:1,000, anti–cyclin B1 monoclonal antibody (BD Biosciences) at 1:1,000, anti–cyclin A polyclonal antibody (Santa Cruz Biotechnology, Inc.) at 1:1,000, anti-Cdc20 polyclonal antibody (Abcam) at 1:300, anti-Cdh1 monoclonal antibody (Calbiochem) at 1:200, antisecurin monoclonal antibody (Abcam) at 1:200, anti-myc (9E10; Sigma-Aldrich), and anti–β-actin polyclonal antibody (Sigma-Aldrich) at 1:10,000.

Immunofluorescence

Cells were plated onto acid-washed glass coverslips. Cells were fixed for 10 min at room temperature in 2% PFA in 1× PBS and for 10 min in methanol at −20°C or in cold methanol alone for 10 min (for the detection of cyclin E). Cells were then permeabilized with PBS-TX (1× PBS + 0.1% Triton X-100) for 15 min followed by incubation in blocking solution (PBS-TX + 1% BSA) at 37°C for 30 min. Coverslips were incubated with primary antibodies diluted in blocking solution overnight at 4°C in a humidity chamber. Secondary antibodies were used at a dilution of 1:250 (Cy2, Rhodamine red-X, or Cy5; Jackson ImmunoResearch Laboratories) and incubated for 1 h at RT. Cells were washed and dehydrated with sequential washes of 70, 90, and 100% ethanol. Coverslips were mounted using SloFade with DAPI (Invitrogen). Primary antibodies used were anti–cyclin E monoclonal antibody (HE12) at 1:1,000, anti–cyclin B1 monoclonal antibody (BD Biosciences) at 1:1,000, antiphosphorylated histone H3 (mitotic marker; Upstate Biotechnology) at 1:400, anti–α-tubulin (Dm1a; Sigma-Aldrich) at 1:1,000, anti-Sm human autosera (centromere-binding protein; gift from K. Sullivan) at 1:100, and sheep polyclonal anti-BrdU (Research Diagnostics, Inc.).

Deconvolution microscopy

Images were collected at intervals of 0.3 μm in the z direction on a widefield optical sectioning microscope system (DeltaVision; Applied Precision) based on an epifluorescence microscope (IX70; Olympus). A 60× or 100× 1.35 NA neofluor oil immersion lens (Olympus) was used. Images were processed using a constrained iterative deconvolution algorithm. All images shown are projections of multiple focal planes, which were created using SoftWoRx analysis software (Applied Precision) and contain information from 3D image stacks.

Live cell microscopy

IME or U2OS cells expressing H2B-GFP were grown directly on glass coverslips. Cells were maintained during imaging in phenol red–free DME plus 10 mM Hepes, pH 7.5, buffer in a closed chamber system (Bioptechs) on a heated stage at 37°C. 5 3-μm sections of differential interference contrast and FITC fluorescence images were acquired at 1-min intervals with a cooled CCD camera mounted on a deconvolution microscope system (DeltaVision; Applied Precision).

Flow cytometry

For flow cytometry, cells were collected by trypsinization, washed with 1× PBS, and fixed with 70% ethanol (added dropwise with agitation) overnight at −20°C. Samples were then washed and resuspended in 1 ml PBS-TX plus 10 μg/ml RNase solution and 2 μg/ml propidium iodide overnight at 4°C. For BrdU staining, cells were pulsed with 10 μM BrdU for 20 min before collection. Cells were treated with 1 ml HCL + 0.5% Triton X-100 for 30 min at RT to denature DNA. The cell suspension was neutralized with 2 ml of 0.1 M Borax. Cells were washed with 1× PBS and resuspended in 50 μl of 1× PBS/1% BSA/0.5% Tween 20 and incubated in 2.5 μg/ml FITC-conjugated anti-BrdU antibody for 1 h at RT. Cells were then washed and incubated with propidium iodide overnight. Before analysis, cells were filtered through a 74-μm mesh (Small Parts) to remove cell clumps before detection on a flow cytometer (FACSCalibur II; Becton Dickinson). For each cell line, 30,000 cells were counted per sample. Data were analyzed using CellQuest (Becton Dickinson). All cell lines were analyzed using the same user-defined Gates and Regions to obtain percentages of cells with a G1, S, or G2/M DNA content.

Thymidine block release protocol for synchronous release into mitosis

KB cells were transduced with EV control or cyclin E adenovirus for 2 h and incubated in medium with 1.5 mM thymidine overnight (∼18 h). Cells were released into S phase and through mitosis by adding 10% FCS medium (with or without 100 nM nocodazole as indicated) after three washes in warm medium. Cells were collected by trypsinization at various time points and split into samples for Western blotting and flow cytometry.

siRNA transfections

siRNAs (21-mers) targeting GFP, Cdh1, securin, and cyclin B (siGENOME; Dharmacon) were used to reduce protein expression in KB cells. Cells were transfected using LipofectAMINE 2000 (12 μl/10-cm dish; Invitrogen) with siRNA (10 pM cyclin B1/securin-specific siRNA, 5 nM Cdh1-specific siRNA, and GFP-specific siRNA up to 20 nM total siRNA concentration or 20 nM GFP-specific siRNA alone). Complexes were incubated for 20 min at RT before adding to cells for 24 h.

Immunoprecipitations and kinase assays

Cell lysates were subjected to immunoprecipitation followed by histone H1 kinase assay or Western blotting. IME or KB cells were lysed in lysis buffer (50 mM Tris, 150 mM NaCl, 1 mM EDTA, 1% Triton X-100 detergent, and phosphatase/protease inhibitors) on ice, sonicated, and cleared for 10 min at 10,000 *g* at 4°C, and protein concentrations were determined using a Bradford solution (Bio-Rad Laboratories) read at 595 nM. For kinase assays, 7.5 μg anti-Cdk2 or IgG1 antibody was added to the lysates with γ-bind G Sepharose beads (100 μl of a 50% slurry; GE Healthcare) for 2 h at 4°C. Beads were washed three to five times with lysis buffer and twice with 1× reaction buffer (without ATP). Beads were resuspended in 2× reaction buffer (40 mM Tris-HCl, pH 7.5, and 15 mM $MgCl_2$), 20 μM ATP, 20 μg histone H1, and 10 μCi γ-[^{32}P]ATP and incubated for 30 min at 37°C. Samples were prepared and run on an 11% SDS-PAGE gel, and autoradiography was performed or phosphorylation was quantified using a phosphorimager (Storm 840; Molecular Dynamics).

Cdh1 kinase assays were performed with 2 μg *E. coli*–purified GST-Cdh1 as a substrate in the kinase reaction. 10 μg GST peptide alone and 2 μg histone H1 kinase assays were used to compared cyclin E/Cdk2 kinase activity.

GST purification of Cdh1 and expression of myc-tagged Cdh1

GST-Cdh1-WT (a gift from C. Sorensen, Danish Cancer Society, Institute of Cancer Biology, Copenhagen, Denmark) had been cloned into the GST-2TK plasmid (GE Healthcare). The fusion protein was expressed in *E. coli* bacteria after induction with IPTG, bound to glutathione–Sepharose beads, and eluted with reduced glutathione. The washes and eluted fractions were run on an SDS-PAGE gel and stained with Coomassie to evaluate purity. GST-Cdh1 was observed running at 75 kD with degradation bands running below.

Myc-tagged Cdh1 constructs (WT, AAA, and 4A or empty vector pX-myc; gifts from C. Sorensen), which were described previously (Sorensen et al., 2001), were expressed in 293T cells along with purified cyclin E or cyclin A using calcium-phosphate transfections and were collected after 48 h of transfection. 9E10 anti-myc antibody (Sigma-Aldrich) was used for immunoprecipitation. Beads were boiled in SDS-running buffer and analyzed by Western blotting. Whole cell lysates and IPs were immunoblotted for cyclin E, cyclin A, or Cdh1.

Cdc27 immunoprecipitations. KB cells were transfected with plasmid expressing myc-tagged Cdh1. 24 h later, cells were transduced with cyclin E–expressing or control adenovirus and subjected to a single thymidine block for 17 h followed by release for 4 h and harvest. Cell pellets were lysed in 50 mM β-glycerophosphate, 5 mM EDTA, 100 mM NaCl, 0.1% Triton X-100, and 1 mM DTT plus protease and phosphatase inhibitors and were cleared by spinning at 15,000 *g* for 15 min. 700 μg lysate was incubated for 1 h with protein A beads coupled to polyclonal antibodies against Cdc27 and then washed three times with lysis buffer. Precipitated proteins were eluted with SDS sample buffer and resolved along with input (50 μg lysates) by SDS-PAGE, transferred to polyvinylidene difluoride membranes, and probed with monoclonal antibodies to Cdh1 (Neomarkers) and Cdc27 (Becton Dickinson). Band densities were measured

with ImageJ software (National Institutes of Health), and ratios of Cdh1/Cdc27 precipitated in each sample were determined and set to 1.0 for the control sample.

Ubiquitylation assays

For kinase inhibition of Cdh1, 2 μl Cdh1 proteins generated with the TNT Quick Coupled Transcription/Translation kit (Promega) with or without ~40 ng cyclin–Cdk2 complexes were diluted in kinase buffer (50 mM Tris, pH 7.5, 10 mM $MgCl_2$, 2 mM DTT, 200 μM ATP, 5 μM okadaic acid, and 1 mM EGTA) to a final reaction volume of 10 μl and incubated at 30°C for 1 h. 100 nM purvalanol A was added to the kinase reactions either before the addition of Cdh1 (with a 15-min preincubation at 30°C) or at the end of the reaction with an additional 15-min incubation to quench the kinase activity.

Anti-Cdc27 polyclonal antibodies coupled to an Affiprep support (Bio-Rad Laboratories) were used to precipitate the APC from interphase *Xenopus laevis* egg extracts. The beads were washed four times in buffer XB^- (20 mM Hepes, pH 7.7, and 100 mM KCl) supplemented with 0.5% NP-40 and 400 mM KCl and then were washed twice in XB^-. Cdh1 proteins were then added to the APC beads and incubated at 4°C for 30 min. The beads were washed twice in XB^- and resuspended in 5 μl of reaction cocktail (20 ng E1, 100 ng UbcH10, and 1.25 μg ubiquitin)/μl in XB^- supplemented with an energy regenerating system and 1 μl ^{35}S-labeled cyclin B1 N-terminal fragment. The reactions were incubated at RT, and samples were taken at the indicated times, resolved by SDS-PAGE, and imaged using a phosphorimager (Typhoon; Molecular Dynamics). Densitometry was performed on the nonmodified substrate using ImageQuant software (Molecular Dynamics). Data was normalized to input and control reactions.

Online supplemental material

Video 1 shows the cyclin E–mediated early mitotic delay presented in Fig. 3 c. Video 2 presents cyclin E–mediated early mitotic delay shown by live cell microscopy in a U2OS cell. Video 3 shows cyclin E–mediated mitotic failure in a U2OS cell. Fig. S1 shows cell cycle analysis of adenovirally expressed cyclin E. Fig. S2 shows a comparison of cyclin E levels during the cell cycle between adenovirally transduced cell lines used in this study and breast cancer–derived cell lines expressing high levels of cyclin E. Fig. S3 shows an analysis of the cyclin E–mediated accumulation of polyploidy cells during one cell cycle equivalent. Online supplemental material is available at http://www.jcb.org/cgi/content/full/jcb.200703202/DC1.

We thank Frank van Drogen for his input and advice. We are grateful to Kevin Sullivan for providing antibodies for immunofluorescence and to Claus Sorensen for providing Cdh1 constructs.

This work was supported by National Institutes of Health (NIH) grant CA78343 to S.I. Reed and grants GM54811 and GM60439 to P.K. Jackson. J.M. Keck was supported by the Department of Defense Predoctoral Fellowship DAMD17-03-1-0383, and M.K. Summers was supported by NIH Tumor Biology Training grant CA09151.

Submitted: 30 March 2007
Accepted: 2 July 2007

References

Arata, Y., M. Fujita, K. Ohtani, S. Kijima, and J.Y. Kato. 2000. Cdk2-dependent and -independent pathways in E2F-mediated S phase induction. *J. Biol. Chem.* 275:6337–6345.

Blanco, M.A., A. Sanchez-Diaz, J.M. de Prada, and S. Moreno. 2000. APC(ste9/srw1) promotes degradation of mitotic cyclins in G(1) and is inhibited by cdc2 phosphorylation. *EMBO J.* 19:3945–3955.

Bortner, D.M., and M.P. Rosenberg. 1997. Induction of mammary gland hyperplasia and carcinomas in transgenic mice expressing human cyclin E. *Mol. Cell. Biol.* 17:453–459.

Brandeis, M., and T. Hunt. 1996. The proteolysis of mitotic cyclins in mammalian cells persists from the end of mitosis until the onset of S phase. *EMBO J.* 15:5280–5289.

Cohen-Fix, O., J.M. Peters, M.W. Kirschner, and D. Koshland. 1996. Anaphase initiation in *Saccharomyces cerevisiae* is controlled by the APC-dependent degradation of the anaphase inhibitor Pds1p. *Genes Dev.* 10:3081–3093.

Dulic, V., E. Lees, and S.I. Reed. 1992. Association of human cyclin E with a periodic G1-S phase protein kinase. *Science*. 257:1958–1961.

Dutta, A., R. Chandra, L.M. Leiter, and S. Lester. 1995. Cyclins as markers of tumor proliferation: immunocytochemical studies in breast cancer. *Proc. Natl. Acad. Sci. USA*. 92:5386–5390.

Ekholm, S.V., and S.I. Reed. 2000. Regulation of G(1) cyclin-dependent kinases in the mammalian cell cycle. *Curr. Opin. Cell Biol.* 12:676–684.

Ekholm-Reed, S., J. Mendez, D. Tedesco, A. Zetterberg, B. Stillman, and S.I. Reed. 2004a. Deregulation of cyclin E in human cells interferes with prereplication complex assembly. *J. Cell Biol.* 165:789–800.

Ekholm-Reed, S., C.H. Spruck, O. Sangfelt, F. van Drogen, E. Mueller-Holzner, M. Widschwendter, A. Zetterberg, and S.I. Reed. 2004b. Mutation of hCDC4 leads to cell cycle deregulation of cyclin E in cancer. *Cancer Res.* 64:795–800.

Erlandsson, F., C. Wahlby, S. Ekholm-Reed, A.C. Hellstrom, E. Bengtsson, and A. Zetterberg. 2003. Abnormal expression pattern of cyclin E in tumour cells. *Int. J. Cancer*. 104:369–375.

Erlanson, M., and G. Landberg. 2001. Prognostic implications of p27 and cyclin E protein contents in malignant lymphomas. *Leuk. Lymphoma*. 40:461–470.

Fang, G., H. Yu, and M.W. Kirschner. 1998. Direct binding of CDC20 protein family members activates the anaphase-promoting complex in mitosis and G1. *Mol. Cell*. 2:163–171.

Geng, Y., Q. Yu, E. Sicinska, M. Das, J.E. Schneider, S. Bhattacharya, W.M. Rideout, R.T. Bronson, H. Gardner, and P. Sicinski. 2003. Cyclin E ablation in the mouse. *Cell*. 114:431–443.

Gimenez-Abian, J.F., L.A. Diaz-Martinez, I.C. Waizenegger, G. Gimenez-Martin, and D.J. Clarke. 2005a. Separase is required at multiple preanaphase cell cycle stages in human cells. *Cell Cycle*. 4:1576–1584.

Gimenez-Abian, J.F., L.A. Diaz-Martinez, K.G. Wirth, C.A. Andrews, G. Gimenez-Martin, and D.J. Clarke. 2005b. Regulated separation of sister centromeres depends on the spindle assembly checkpoint but not on the anaphase promoting complex/cyclosome. *Cell Cycle*. 4:1561–1575.

Gorr, I.H., D. Boos, and O. Stemmann. 2005. Mutual inhibition of separase and Cdk1 by two-step complex formation. *Mol. Cell*. 19:135–141.

Harbour, J.W., R.X. Luo, A. Dei Santi, A.A. Postigo, and D.C. Dean. 1999. Cdk phosphorylation triggers sequential intramolecular interactions that progressively block Rb functions as cells move through G1. *Cell*. 98:859–869.

Hauf, S., I.C. Waizenegger, and J.M. Peters. 2001. Cohesin cleavage by separase required for anaphase and cytokinesis in human cells. *Science*. 293:1320–1323.

Hendzel, M.J., Y. Wei, M.A. Mancini, A. Van Hooser, T. Ranalli, B.R. Brinkley, D.P. Bazett-Jones, and C.D. Allis. 1997. Mitosis-specific phosphorylation of histone H3 initiates primarily within pericentromeric heterochromatin during G2 and spreads in an ordered fashion coincident with mitotic chromosome condensation. *Chromosoma*. 106:348–360.

Hubalek, M.M., A. Widschwendter, M. Erdel, A. Gschwendtner, H.M. Fiegl, H.M. Muller, G. Goebel, E. Mueller-Holzner, C. Marth, C.H. Spruck, et al. 2004. Cyclin E dysregulation and chromosomal instability in endometrial cancer. *Oncogene*. 23:4187–4192.

Jaspersen, S.L., J.F. Charles, and D.O. Morgan. 1999. Inhibitory phosphorylation of the APC regulator Hct1 is controlled by the kinase Cdc28 and the phosphatase Cdc14. *Curr. Biol.* 9:227–236.

Jeganathan, K.B., L. Malureanu, and J.M. van Deursen. 2005. The Rae1-Nup98 complex prevents aneuploidy by inhibiting securin degradation. *Nature*. 438:1036–1039.

Jeganathan, K.B., D.J. Baker, and J.M. van Deursen. 2006. Securin associates with APCCdh1 in prometaphase but its destruction is delayed by Rae1 and Nup98 until the metaphase/anaphase transition. *Cell Cycle*. 5:366–370.

Ji, J.Y., J. Crest, and G. Schubiger. 2005. Genetic interactions between Cdk1-CyclinB and the Separase complex in *Drosophila*. *Development*. 132:1875–1884.

Kanda, T., K.F. Sullivan, and G.M. Wahl. 1998. Histone-GFP fusion protein enables sensitive analysis of chromosome dynamics in living mammalian cells. *Curr. Biol.* 8:377–385.

Keyomarsi, K., D. Conte Jr., W. Toyofuku, and M.P. Fox. 1995. Deregulation of cyclin E in breast cancer. *Oncogene*. 11:941–950.

Keyomarsi, K., S.L. Tucker, T.A. Buchholz, M. Callister, Y. Ding, G.N. Hortobagyi, I. Bedrosian, C. Knickerbocker, W. Toyofuku, M. Lowe, et al. 2002. Cyclin E and survival in patients with breast cancer. *N. Engl. J. Med.* 347:1566–1575.

Knoblich, J.A., K. Sauer, L. Jones, H. Richardson, R. Saint, and C.F. Lehner. 1994. Cyclin E controls S phase progression and its down-regulation during *Drosophila* embryogenesis is required for the arrest of cell proliferation. *Cell*. 77:107–120.

Koff, A., F. Cross, A. Fisher, J. Schumacher, K. Leguellec, M. Philippe, and J.M. Roberts. 1991. Human cyclin E, a newe cyclin that interacts with two members of the CDC2 gene family. *Cell*. 66:1217–1228.

Kramer, E.R., N. Scheuringer, A.V. Podtelejnikov, M. Mann, and J.M. Peters. 2000. Mitotic regulation of the APC activator proteins CDC20 and CDH1. *Mol. Biol. Cell*. 11:1555–1569.

Lukas, C., C.S. Sorensen, E. Kramer, E. Santoni-Rugiu, C. Lindeneg, J.M. Peters, J. Bartek, and J. Lukas. 1999. Accumulation of cyclin B1 requires E2F and cyclin-A-dependent rearrangement of the anaphase-promoting complex. *Nature*. 401:815–818.

Lukas, J., T. Herzinger, K. Hansen, M.C. Moroni, D. Resnitzky, K. Helin, S.I. Reed, and J. Bartek. 1997. Cycline E-induced S phase without activation of the pRb/E2F pathway. *Genes Dev.* 11:1479–1492.

Mailand, N., and J.F. Diffley. 2005. CDKs promote DNA replication origin licensing in human cells by protecting Cdc6 from APC/C-dependent proteolysis. *Cell*. 122:915–926.

Morgenstern, J.P., and H. Land. 1990. Advanced mammalian gene transfer: high titre retroviral vectors with multiple drug selection markers and a complementary helper-free packaging cell line. *Nucleic Acids Res.* 18:3587–3596.

Nielsen, N.H., C. Arnerlov, S. Cajander, and G. Landberg. 1998. Cyclin E expression and proliferation in breast cancer. *Anal. Cell. Pathol.* 17:177–188.

Ohtsubo, M., and J.M. Roberts. 1993. Cyclin-dependent regulation of G1 in mammalian fibroblasts. *Science*. 259:1908–1912.

Ohtsubo, M., A.M. Theodoras, J. Schumacher, J.M. Roberts, and M. Pagano. 1995. Human cyclin E, a nuclear protein essential for the G1-to-S phase transition. *Mol. Cell. Biol.* 15:2612–2624.

Porter, P.L., K.E. Malone, P.J. Heagerty, G.M. Alexander, L.A. Gatti, E.J. Firpo, J.R. Daling, and J.M. Roberts. 1997. Expression of cell-cycle regulators p27Kip1 and cyclin E, alone and in combination, correlate with survival in young breast cancer patients. *Nat. Med.* 3:222–225.

Rajagopalan, H., P.V. Jallepalli, C. Rago, V.E. Velculescu, K.W. Kinzler, B. Vogelstein, and C. Lengauer. 2004. Inactivation of hCDC4 can cause chromosomal instability. *Nature*. 428:77–81.

Resnitzky, D., M. Gossen, H. Bujard, and S.I. Reed. 1994. Acceleration of the G1/S phase transition by expression of cyclins D1 and E with an inducible system. *Mol. Cell. Biol.* 14:1669–1679.

Salah, S.M., and K. Nasmyth. 2000. Destruction of the securin Pds1p occurs at the onset of anaphase during both meiotic divisions in yeast. *Chromosoma*. 109:27–34.

Sandhu, C., and J. Slingerland. 2000. Deregulation of the cell cycle in cancer. *Cancer Detect. Prev.* 24:107–118.

Sauer, K., and C.F. Lehner. 1995. The role of cyclin E in the regulation of entry into S phase. *Prog. Cell Cycle Res.* 1:125–139.

Sigrist, S.J., and C.F. Lehner. 1997. *Drosophila* fizzy-related down-regulates mitotic cyclins and is required for cell proliferation arrest and entry into endocycles. *Cell*. 90:671–681.

Sigrist, S., H. Jacobs, R. Stratmann, and C.F. Lehner. 1995. Exit from mitosis is regulated by *Drosophila* fizzy and the sequential destruction of cyclins A, B and B3. *EMBO J.* 14:4827–4838.

Smith, A.P., M. Henze, J.A. Lee, K.G. Osborn, J.M. Keck, D. Tedesco, D.M. Bortner, M.P. Rosenberg, and S.I. Reed. 2006. Deregulated cyclin E promotes p53 loss of heterozygosity and tumorigenesis in the mouse mammary gland. *Oncogene*. 25:7245–7259.

Sorensen, C.S., C. Lukas, E.R. Kramer, J.M. Peters, J. Bartek, and J. Lukas. 2000. Nonperiodic activity of the human anaphase-promoting complex-Cdh1 ubiquitin ligase results in continuous DNA synthesis uncoupled from mitosis. *Mol. Cell. Biol.* 20:7613–7623.

Sorensen, C.S., C. Lukas, E.R. Kramer, J.M. Peters, J. Bartek, and J. Lukas. 2001. A conserved cyclin-binding domain determines functional interplay between anaphase-promoting complex-Cdh1 and cyclin A-Cdk2 during cell cycle progression. *Mol. Cell. Biol.* 21:3692–3703.

Spruck, C.H., K.-A. Won, and S.I. Reed. 1999. Deregulated cyclin E induces chromosome instability. *Nature*. 401:297–300.

Spruck, C.H., H. Strohmaier, O. Sangfelt, H.M. Muller, M. Hubalek, E. Muller-Holzner, C. Marth, M. Widschwendter, and S.I. Reed. 2002. hCDC4 gene mutations in endometrial cancer. *Cancer Res.* 62:4535–4539.

Strohmaier, H., C.H. Spruck, P. Kaiser, K.-A. Won, O. Sangfelt, and S.I. Reed. 2001. Human F-box protein hCdc4 targets cyclin E for proteolysis and is mutated in a breast cancer cell line. *Nature*. 413:316–322.

Thiagalingam, S., S. Laken, J.K.V. Willson, S.D. Markowitz, K.W. Kinzler, B. Vogelstein, and C. Lengauer. 2000. Mechanisms underlying losses of heterozygosity in human colorectal cancers. *Proc. Natl. Acad. Sci. USA*. 98:2698–2702.

Uhlmann, F., F. Lottspeich, and K. Nasmyth. 1999. Sister-chromatid separation at anaphase onset is promoted by cleavage of the cohesin subunit Scc1. *Nature*. 400:37–42.

Uhlmann, F., D. Wernic, M.A. Poupart, E.V. Koonin, and K. Nasmyth. 2000. Cleavage of cohesin by the CD clan protease separin triggers anaphase in yeast. *Cell*. 103:375–386.

Visintin, R., S. Prinz, and A. Amon. 1997. CDC20 and CDH1: a family of substrate-specific activators of APC-dependent proteolysis. *Science*. 278:460–463.

Waizenegger, I.C., S. Hauf, A. Meinke, and J.M. Peters. 2000. Two distinct pathways remove mammalian cohesin from chromosome arms in prophase and from centromeres in anaphase. *Cell*. 103:399–410.

Waizenegger, I., J.F. Gimenez-Abian, D. Wernic, and J.M. Peters. 2002. Regulation of human separase by securin binding and autocleavage. *Curr. Biol.* 12:1368–1378.

Zachariae, W., M. Schwab, K. Nasmyth, and W. Seufert. 1998. Control of cyclin ubiquitination by CDK-regulated binding of Hct1 to the anaphase promoting complex. *Science*. 282:1721–1724.

Zhang, H.S., A.A. Postigo, and D.C. Dean. 1999. Active transcriptional repression by the Rb-E2F complex mediates G1 arrest triggered by p16INK4a, TGFbeta, and contact inhibition. *Cell*. 97:53–61.

Zou, H., T.J. McGarry, T. Bernal, and M.W. Kirschner. 1999. Identification of a vertebrate sister-chromatid separation inhibitor involved in transformation and tumorigenesis. *Science*. 285:418–422.

Zur, A., and M. Brandeis. 2001. Securin degradation is mediated by fzy and fzr, and is required for complete chromatid separation but not for cytokinesis. *EMBO J.* 20:792–801.